Triarylphosphine Ligands with Pendant Electron-Rich "[Fe(κ²-dppe)(η⁵-C₅Me₅)(C≡C)]−" Substituents
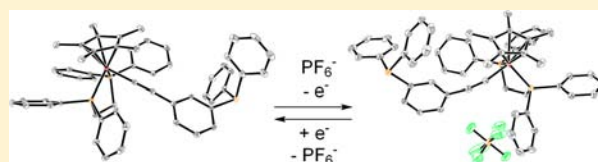
Ayham Tohmé,[†] Guillaume Grelaud,[†] Gilles Argouarch,[†] Thierry Roisnel,[†] Arnaud Bondon,[‡] and Frédéric Paul*,[†]

[†]Institut des Sciences Chimiques de Rennes-UMR CNRS 6226, Université de Rennes 1, Campus de Beaulieu, 35042 Rennes Cedex, France

[‡]SIM-UMR CNRS 6290, Université de Rennes 1, PRISM-Biosit-CS 34317, Campus de Villejean, 35043 Rennes Cedex, France

⑤ Supporting Information

ABSTRACT: The synthesis of four triaylphosphine ligands featuring electron-rich Fe(II) "Fe(κ²-dppe)(η⁵-C₅Me₅)C≡C−" pendant substituents in *para* and *meta* position(s) (**1−4**) is reported along with that of their corresponding radical cations (**1−2**[PF₆] or **3−4**[PF₆]₃). These triarylphosphines possessing redox-active organometallic substituents constitute a new class of phosphorus-based metallo-ligands. In contrast to many related ferrocenylphosphines, these metallo-ligands are stable and isolable in two redox-states. Their steric and electronic properties are also briefly discussed.

INTRODUCTION

Judicious spatial or topologic arrangements of redox-active end groups can lead to molecular architectures presenting unique properties for information storage or processing at the molecular level.[1] Accordingly, ferrocene-containing ligands have attracted a strong attention in the organometallic scientific community very early for the realization of molecular-based devices.[2,3] Likewise, we[4−7] and others[8] became interested in introducing the redox-active "Fe(κ²-dppe)(η⁵-C₅Me₅)(C≡C−)" fragment in several classes of ubiquitous ligands.[9] When appended to an (hetero)aromatic ring, this organoiron fragment usually presents a chemically reversible oxidation at rather accessible potentials (around −0.1 V vs SCE)[10] and, depending on its redox state, was shown to interact more or less strongly with this unit,[5] opening access to various devices such as self-assembled molecular wires.[7,11]

In the continuation of our studies aimed at developing organoiron-based *metallo*-ligands, we have recently turned our attention toward triarylphosphines such as **1−4** and briefly communicated on their use in catalysis (Scheme 1).[12] Indeed, given the strong implication of triarylphosphines in many catalytic transformations,[13] the possibility of using the redox state of "Fe(κ²-dppe)(η⁵-C₅Me₅)(C≡C−)" substituents of **1−4** to switch/modulate one of these transformations constitutes an additional incentive to study such derivatives.[14] However, the redox-control of a catalytic transformation represents a challenging goal only seldom met with redox-active phosphine-based ligands.[15] Although several phosphine ligands functionalized with *electron-rich* organometallics have been designed for catalysis,[16−22] only few among these ligands have been studied in their oxidized states.[18−21,23−25] In spite of these developments, phosphines functionalized with redox-active metal-alkynyl substituents (**5−7**) remain scarce,[26−28] and **5**, the

only *triaryl*phosphine representative reported to date, exhibits a chemically irreversible Ru(II/III) oxidation in cyclic voltammetry (CV).[26,29] In this respect, **1−4** appear quite promising for redox-controlling chemical transformations, since **1−4** are reversibly oxidized at much lower potentials than **5**, but also than most of the known metallo-phosphines. Considering the fair kinetic stability reported for almost all arylalkynyl Fe(III) complexes such as **8-X** (Scheme 1),[30,31] a comparably better kinetic stability can be expected for the cationic species **1⁺−4³⁺**.[32] Moreover, the recent demonstration that the neutral precursors **1−4** can behave as active ligands in a given catalytic transformation certainly warrants further interest for these derivatives.[12]

Accordingly, we now report here *(i)* a full account of the synthesis and characterization of the new metallo-ligands **1−4**[PF₆]ₙ in their neutral (*n* = 0) and cationic (*n* = 1 or 3) redox states, *(ii)* the study of the electronic effect induced by the Fe(II)-based oxidations on Rh(I) carbonyl complexes of **1** and **2** to quantify the effect of the perturbation induced by oxidation on the terminal phosphorus atom, and *(iii)* a brief discussion of their electronic and steric parameters in relation to these reported for related metallo-phosphines.

RESULTS

Synthesis and Characterization of the Fe(II) Metallophosphines. The organometallic ligands **1−4** were synthesized from the corresponding organic phosphine precursors presenting peripheral alkyne groups **9−12**[33] and from the Fe(II) chloride complex Fe(κ²-dppe)(η⁵-C₅Me₅)Cl (**13**) in two steps, following a classic activation-deprotonation

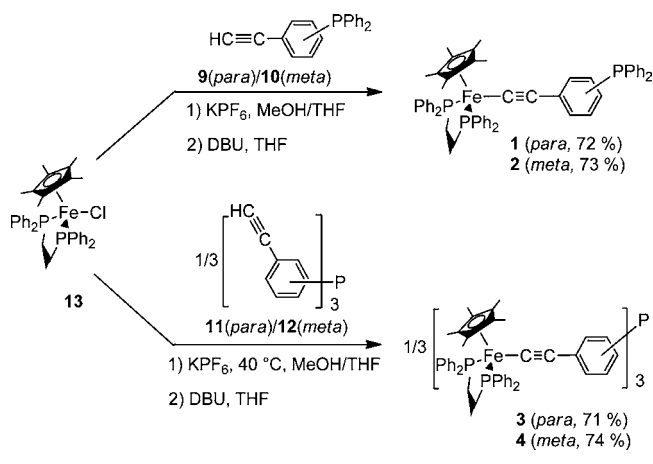**Scheme 1. New Fe(II) Metallo-Ligands 1−4 and Related Metallo-Phosphines and Metal-Alkynyl Complexes (Inset).**
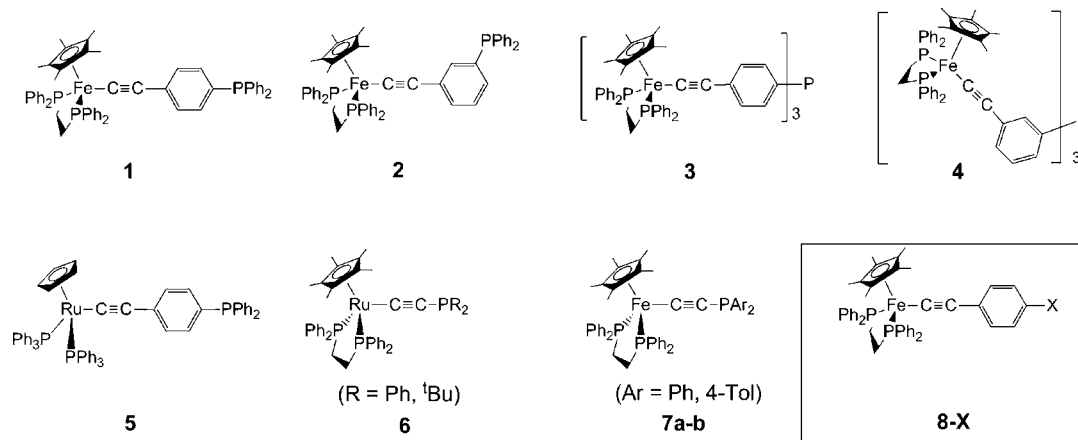
reaction which has ample precedence in our group (Scheme 2).[34,35] While the mono- or tris-cationic vinylidene complexes

Scheme 2. Synthesis of the Fe(II) Metallophosphines 1−4

Table 1. Characteristic Spectroscopic and Redox Signatures of the Fe(II) Metalloligands 1−4, Their Rh(I) Complexes 15 and 16, and 8-H

entry	δ_{dppe} (ppm)[a]	δ_P (ppm)[a]	$\nu_{C\equiv CFe}$ (cm^{-1})[b,c]	$E°$ [ΔE_p] (V)[d,e]
PPh$_3$		−5.5		
1	100.1	−5.4	2048 (vs), 2018 (m)	−0.14 [0.08]
2	100.1	−5.9	2068 (m), 2034 (vs)	−0.15 [0.08]
3	100.3	−5.3	2048 (vs), 2015 (sh)	−0.12 [0.12]
4	100.1	−3.8	2068 (sh), 2035 (vs)	−0.13 [0.18]
8-H	101.7		2053 (s)	−0.15 [0.08]
15	100.0	28.7[f,g]	2043 (s), 2022 (sh)	−0.10 [0.13]
16	100.0	29.5[f,g]	2039 (s)	−0.13 [0.11]

[a] ^{31}P{^{1}H} NMR in C$_6$D$_6$ (±0.2 ppm). [b] IR in KBr pellets (±2 cm^{-1}). [c] In most cases two $\nu_{C\equiv C}$ modes are reported. These are presumably due to Fermi coupling.[38] [d] Values in V (±5 mV) vs SCE. Conditions: CH$_2$Cl$_2$ solvent, 0.1 M [^{n}Bu$_4$N][PF$_6$] supporting electrolyte, 20 °C, Pt electrodes, sweep rate 0.100 V s^{-1}. [e] ΔE_p represents the peak-to-peak separation in V. [f] $^1J_{PRh}$ = 127 Hz. [g] A ^{31}P NMR signal is observed at δ_P = 29.0 ppm (d, $^1J_{PRh}$ = 127 Hz) for the reference compound [Rh(Ph$_3$P)$_2$(CO)Cl] (**17**) under similar conditions.

(vin-**1**[PF$_6$]/vin-**2**[PF$_6$]/vin-**3**[PF$_6$]$_3$/vin-**4**[PF$_6$]$_3$), isolated as intermediates during the synthesis, were only briefly characterized (NMR), the final alkynyl complexes were fully characterized. For the latter, NMR and IR are plainly diagnostic of the presence of Fe(II) metal-alkynyl substituents on the aryl groups of the phosphines (Table 1). The compounds **1**−**3** were also characterized by X-ray diffraction (Figure 1).

These orange complexes are redox-active and present a chemically reversible Fe(III)/Fe(II) metal-centered oxidation near −0.15 V vs SCE (Table 1).[34] The PPh$_2$ substituent in the monometallic derivatives **1** and **2** plays the role of a weakly electron-attracting substituent, as evidenced by the higher oxidation potential and the slightly lower $\nu_{C\equiv C}$ values compared to Fe(κ^2-dppe)(η^5-C$_5$Me$_5$)(C≡CPh) (**8-H**).[36] Expectedly, this effect is slightly stronger for the *para*- than for the *meta*-substituted Fe(II) complex. The corresponding trimetallic complexes **3** and **4** also exhibit a single and broader redox wave, corresponding to the simultaneous oxidation of the three organoiron end groups at slightly higher redox potentials values than for the monometallic derivatives **1** and **2**. The observation of a single oxidation wave for the three redox-active units in the trinuclear structures is indicative of virtually no electronic coupling between these units. Also, a single but broader absorption band is observed by IR spectroscopy for the

overlapping E and A$_1$ $\nu_{C\equiv C}$ modes of **1** and **2** which are both in principle infrared active.[37] This absorption is observed at roughly the same energy than for the corresponding monometallic complexes, in line with a weak (or null) vibronic coupling between the alkynyl stretching motions.

Synthesis and Characterization of the Fe(III) Metallophosphines. The Fe(III) complexes were synthesized by chemical oxidation using one equivalent of ferrocenium hexafluorophosphate per organoiron end-group, and readily isolated in good to excellent yields by reprecipitation of the crude solid from dichloromethane/n-pentane (Scheme 3). The CVs of **1**[PF$_6$]−**4**[PF$_6$]$_3$ remained identical to those of the starting Fe(II) complexes with the sign of the initial current changing from anodic to cathodic, indicating the absence of decomposition and/or the formation of new electroactive side-products, while observation of characteristic spectroscopic signatures evidences that the targeted Fe(III) complexes have indeed been isolated (Table 2). For instance, the IR showed the characteristic shift toward lower wave numbers of the $\nu_{C\equiv CFe}$ stretching mode(s) (Table 2).[31,38] The compound **2**[PF$_6$] could also be characterized by its solid state structure (Figure 2).
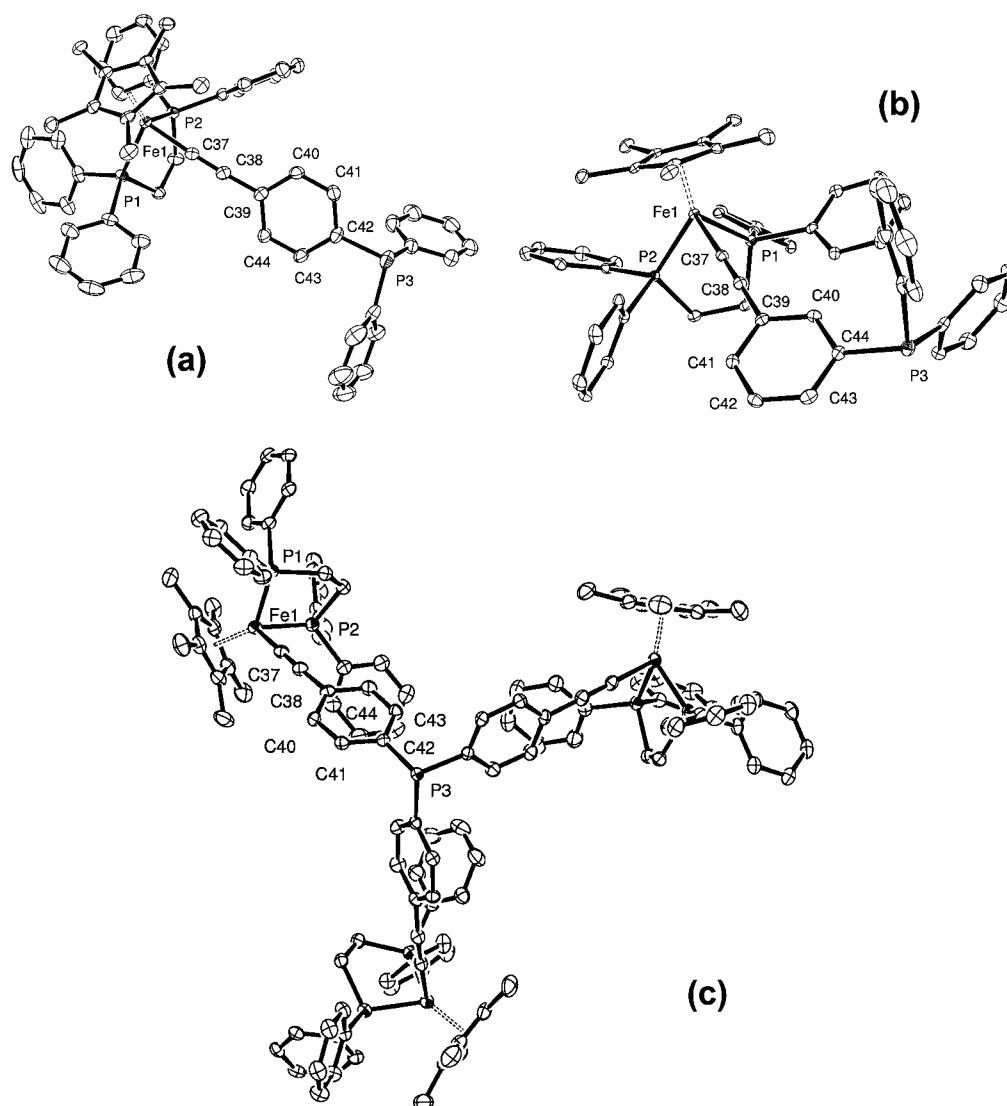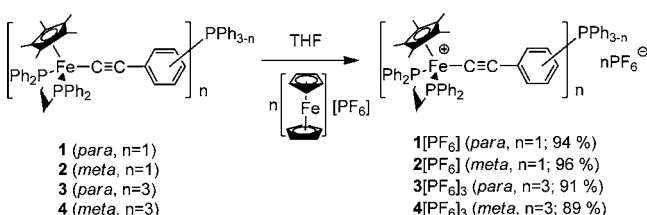
Figure 1. ORTEP representations of the complexes **1** (a), **2** (b), and **3** (c) with displacement ellipsoids at the 50% probability level. Selected distances (Å) and angles (deg): (a) Fe1−(Cp*)$_{\text{centroid}}$ 1.740, Fe1−P1 2.1705(5), Fe1−P2 2.1750(5), Fe1−C37 1.8893(17), C37−C38 1.222(2), C38−C39 1.437(2), C42−P3 1.8315(18), P1−Fe1−P2 85.638(19), Fe1−C37−C38 176.96(16), C37−C38−C39 177.37(19), C40−C39−Fe1−(Cp*)$_{\text{centroid}}$ −52.3; (b) Fe1−(Cp*)$_{\text{centroid}}$ 1.736, Fe1−P1 2.1893(7), Fe1−P2 2.1821(7), Fe1−C37 1.906(2), C37−C38 1.221(3), C38−C39 1.440(3), C44−P3 1.838 (3), P1−Fe1−P2 86.20(2), Fe1−C37−C38 178.0(2), C37−C38−C39 176.7(2), C40−C39−Fe1−(Cp*)$_{\text{centroid}}$ −77.6; (c) Fe1−(Cp*)$_{\text{centroid}}$ 1.741, Fe1−P1 2.1794(6), Fe1−P2 2.1832(6), Fe1−C37 1.882(2), C37−C38 1.220(3), C38−C39 1.432(3), C42−P3 1.8241(19), P1−Fe1−P2 84.99(2), Fe1−C37−C38 176.56(19), C37−C38−C39 169.2(2), C42−P3−C42 103.00(7), C40−C39−Fe1−(Cp*)$_{\text{centroid}}$ −24.9.

Scheme 3. Synthesis of the Fe(III) Metallophosphines 1[PF$_6$]−4[PF$_6$]$_3$

1 (*para*, n=1)
2 (*meta*, n=1)
3 (*para*, n=3)
4 (*meta*, n=3)

1[PF$_6$] (*para*, n=1; 94 %)
2[PF$_6$] (*meta*, n=1; 96 %)
3[PF$_6$]$_3$ (*para*, n=3; 91 %)
4[PF$_6$]$_3$ (*meta*, n=3; 89 %)

As evidenced by rhombic electron spin resonance (ESR) signatures in solvent glasses at about 77 K, the monocations **1**[PF$_6$] and **2**[PF$_6$] are typical Fe(III) metallo-centered radicals (Table 2).[10] The slight change in anisotropy (Δg) and mean g value ($\langle g \rangle$) observed between them being attributable to the higher electron-withdrawing capability of the PPh$_2$ substituent

when placed in *para*-position on the ring.[31] In comparison, the trications give much broader and apparently more isotropic signals at about the same g values, a feature likely attributable to their tri-radical nature inducing a faster spin relaxation, possibly because of intramolecular spin−spin interactions.[39,40]

The $\nu_{\text{C}\equiv\text{CFe}}$ shifts observed for **1**[PF$_6$] and **2**[PF$_6$] and for the corresponding trications **3**[PF$_6$]$_3$ and **4**[PF$_6$]$_3$ are comparable to these previously observed for closely related Fe(III) complexes (Table 2).[38] They suggest a weakening of the alkynyl bond order upon oxidation because of some delocalization of the electronic vacancy on the nearby phenyl ring and perhaps even on the phosphorus lone pair, based on π-conjugation effects.[31] Indeed, in line with VB considerations, the observed bond weakening is larger in the *para*- than in the *meta*-substituted triarylphosphines. Finally, a weak signal in the near-IR range corresponding to a forbidden LF transition can be detected for all these compounds,[31] with roughly a 3-fold

Table 2. Characteristic Spectroscopic Signatures of the Fe(III) Metallo-Ligands $1[PF_6]-4[PF_6]_3$

entry	$\nu_{C\equiv C}$ (cm^{-1})[a]	λ_{LF} (nm)[d]	g_1[e]	g_2[e]	g_3[e]	Δg	$\langle g \rangle$
$1[PF_6]$	1993	1879 (0.08)	1.969	2.027	2.495	0.526	2.164
$2[PF_6]$	2000	1857 (0.11)	1.972	2.027	2.470	0.498	2.156
$8\text{-}H[PF_6]$	2021/1988[b]	1846 (0.09)	1.975	2.033	2.464	0.489	2.157
$15[PF_6]_2$	2025/2007[b,c]	1884 (0.21)	1.978	2.033	2.474	0.496	2.162
$16[PF_6]_2$	2022/2010[b,c]	1861 (0.14)	1.976	2.032	2.472	0.496	2.160
			g[e]			ΔH_{PP}[f] (Hz)	
$3[PF_6]_3$	1988	1863 (0.34)	2.116			445	
$4[PF_6]_3$	2000	1863 (0.32)	2.137			377	

[a]IR in KBr pellets (2 cm^{-1}). [b]Two bands were observed for the Fe(III) parent, presumably due to Fermi coupling.[38] [c]Determined by Raman spectroscopy because of their weak intensity in the IR range. [d]UV−vis−near-IR in CH$_2$Cl$_2$ ($10^{-3} \times \varepsilon$ in M^{-1} cm^{-1}). [e]ESR of Fe(III) complex at ca. 77 K in CH$_2$Cl$_2$/1,2-C$_2$H$_4$Cl$_2$ (1:1) glass. [f]Peak-to-peak separation.
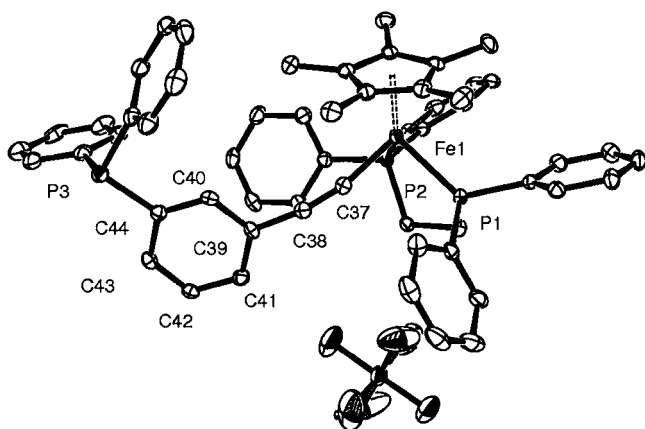

Figure 2. ORTEP representation of the complex $2[PF_6]$ with displacement ellipsoids at the 50% probability level. Selected distances (Å) and angles (deg): Fe1−(Cp*)$_{centroid}$ 1.780, Fe1−P1 2.2780(9), Fe1−P2 2.2545(9), Fe1−C37 1.879(3), C37−C38 1.221(4), C38−C39 1.430(4), C44−P3 1.848(3), P1−Fe1−P2 84.71(3), Fe1−C37−C38 167.1(3), C37−C38−C39 169.3(3), C40−C39−Fe1−(Cp*)$_{centroid}$ 20.3.

intensity for the trinuclear derivatives corresponding to the increased number of Fe(III) chromophores in $3[PF_6]_3$ and $4[PF_6]_3$. In full accordance with the available ESR data (Table 2), the energies of these transitions in $1[PF_6]$ and $2[PF_6]$, as well as those of their first LMCT bands relative to the corresponding bands in $8\text{-}H[PF_6]$ are indicative of the weakly electron-withdrawing nature of the PPh$_2$ substituent.[31]

^{1}H NMR of the Fe(III) Metallophosphines. These paramagnetic species were also characterized in solution by NMR.[30,40] They give well-resolved spectra in which the shift of all their protons can be identified by analogy with those of related complexes, supplemented by integration and, whenever possible, by polarization transfer experiments. Such an approach leads to an unambiguous assignment of all the observed signals of $1[PF_6]-4[PF_6]_3$. Regardless of their mono- ($1[PF_6]-2[PF_6]$) or trinuclear ($3[PF_6]_3-4[PF_6]_3$) nature, the ^{1}H NMR shifts of the "Fe(κ^2-dppe)(η^5-C$_5$Me$_5$)" end-groups are quasi-unchanged from one Fe(III) complex to the other, with the various proton signals coming out at classical shift values.[30] Thus, while the spectra of the trications are fairly similar (see Supporting Information), they differ from these of the monocations, which are also different from each other (Figure 3). These changes mostly originate from the protons of the three phenyl groups bound to the phosphorus atom. The isotropic shifts of these nuclei remote from the Fe(III) center

are certainly dominated by the so-called contact contribution which reflects the changes in spin polarization along the backbone of the unsaturated carbon-rich ligand.[30,41] Thus, given that the signals corresponding to H$_1$, H$_{1'}$, and H$_{1''}$ (Chart 1) accidentally overlap for $2[PF_6]$ and come close together for $4[PF_6]_3$, the changes in the bridging phenylene group when proceeding from $1[PF_6]$ to $2[PF_6]$ essentially translate in a change in intensity of the most shifted signals of the spectrum at high and low fields (Figure 3). The most notable difference between these two Fe(III) complexes originate from the phenyl protons of the terminal PPh$_2$ groups, absent on the trications $3[PF_6]_3$ and $4[PF_6]_3$, but readily identified for $1[PF_6]$ and $2[PF_6]$ by polarization transfer experiments (See Supporting Information). The spin polarization being of opposite sign depending on whether the PPh$_2$ substituent is positioned in *meta*- or *para*- position relative to the Fe(III)-C≡C- arm on the ring,[42] the *ortho/para* and *meta* sets of protons of the terminal phenyl rings are thus shifted in opposite directions from their position in the diamagnetic Fe(II) complex (near 7.5 ppm). This shift, albeit weak, results in a characteristic inversion of these sets of signals in $1[PF_6]$ and $2[PF_6]$.

Given that the broadened ESR spectra of the tricationic species $3[PF_6]_3$ and $4[PF_6]_3$ were suggestive of some spin−spin interactions, we wondered if any sizable intramolecular exchange interactions was taking place between the unpaired spins in these triradical species, as was the case with the related triarylamine compound **14** recently studied by some of us (Scheme 5).[43] However, the fact that the protons H$_1$ and H$_2$ (Chart 1) appear nearly as shifted in $3[PF_6]_3$ than in $1[PF_6]$ suggests that the electronic environment of the unpaired spins in the *para*-substituted trication and in the corresponding monocation are not so different in solution at room temperature, in line with a weak to negligible exchange coupling between them in the trications.[42] A simple means to confirm the existence of significant antiferromagnetic interactions is to monitor the temperature dependence of the most shifted protons of these Fe(III) derivatives.[42] The clear Curie dependence of these shifts with temperature for both $3[PF_6]_3$ and $4[PF_6]_3$ (Supporting Information) in the range accessible for dichloromethane (20 to −90 °C) reveals that if any such exchange interaction is taking place, the latter must be quite weak, and is anyway not significantly larger than that taking place in the related arylamine complexes previously mentioned (mean $J_{FeFe} \sim 14$ cm^{-1}).

Synthesis of Rhodium(I) Carbonyl Complexes. Rhodium carbonyl complexes of **1** and **2** were synthesized by reacting these ligands with the dimeric Rh(I) precursor [Rh(CO)$_2$Cl]$_2$ (Scheme 4).[44,45] The square planar carbonyl
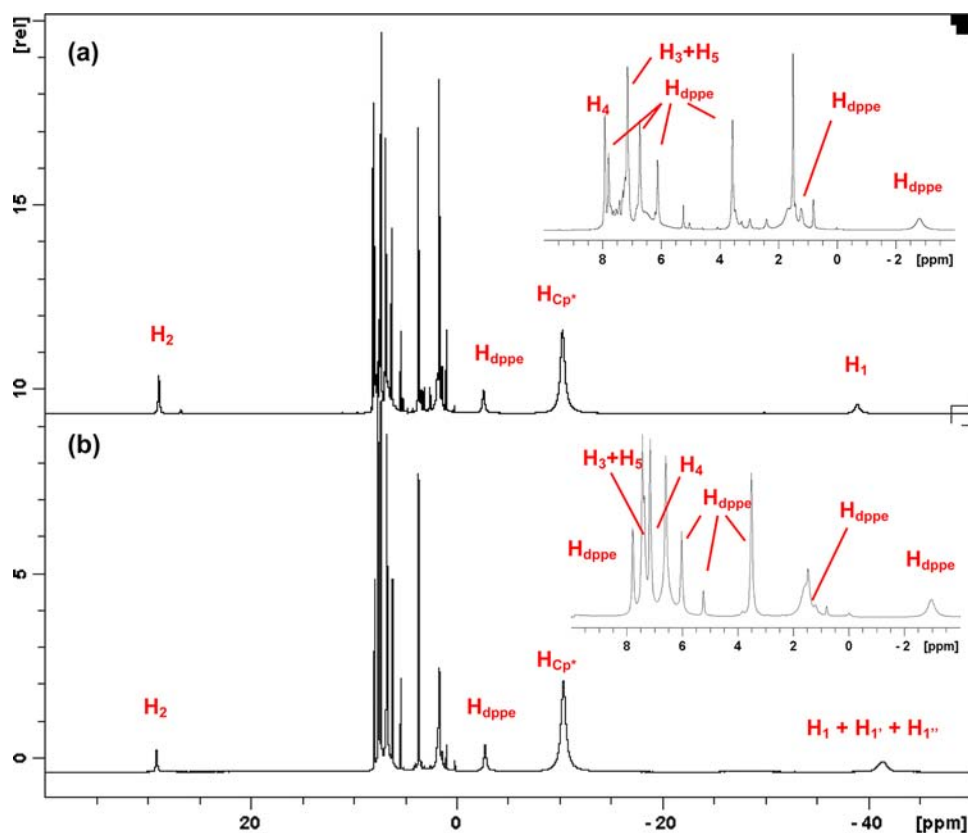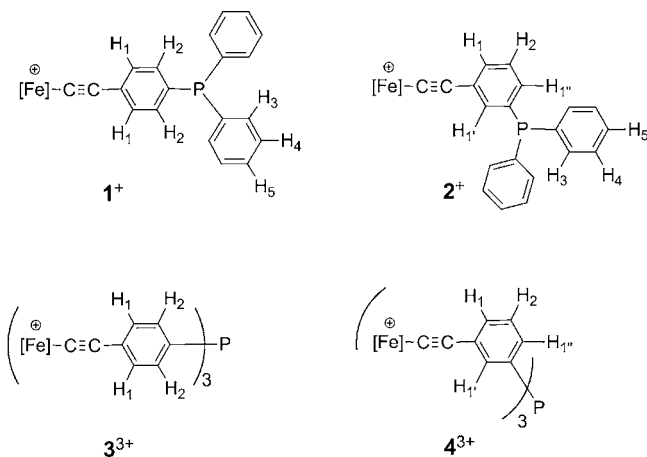
Figure 3. ^{1}H NMR spectra of **1**[PF$_6$] (a) and **2**[PF$_6$] (b) in CD$_2$Cl$_2$ at 25 °C with proposed assignment according to Chart 1 for selected protons. Specific assignment of protons in the diamagnetic range are given on scaled up spectra. Unlabeled signals correspond to residual solvent peaks.

Chart 1. Labeling of Selected Protons of 1[PF$_6$], 2[PF$_6$], 3[PF$_6$]$_3$, and 4[PF$_6$]$_3$ ([Fe] = Fe(κ^2-dppe)(η^5-C$_5$Me$_5$))

and **16** with two equivalents of ferrocenium hexafluorophosphate in dichloromethane. IR, UV−vis and ^{1}H NMR spectroscopies, combined with cyclic voltammetry of the isolated species **15**[PF$_6$]$_2$ and **16**[PF$_6$]$_2$ indicate that no dissociation of the oxidized ligands takes place subsequent to oxidation (Table 2). The characterization of all these Rh(I) complexes was then complemented by Raman spectroscopy to firmly identify the carbonyl stretching frequencies (Table 3). Indeed, we have found that the stretching motion of the strongly polarized carbonyl bond was not active in Raman, allowing for a clear identification of the latter mode in infrared where both the $\nu_{C\equiv C}$ and ν_{CO} modes proved to be active. The ν_{CO} mode in **15**[PF$_6$]$_n$−**16**[PF$_6$]$_n$ (n = 0, 2) is always observed at marginally higher values than that of the reference compound [Rh(Ph$_3$P)$_2$(CO)Cl] (**17**).[46]

Crystallography. We report the solid-state structures of the Fe(II) complexes **1**, **2**, and **3** (Figure 1), along with that of the Fe(III) complex **2**[PF$_6$] (Figure 2) and of the Rh(I) complex **15** (Figure 4). As often observed, the mononuclear complexes **1**, **2**, and **2**[PF$_6$] crystallize in mono- or triclinic systems, in centrosymmetric space groups. In this respect, the trinuclar Fe(II) complex is more original since it crystallizes in a trigonal system, in the $R\overline{3}$ space group (Table 4). Both distances and angles values are classical for Fe(II)[6,31,34,36,39,43,55,56] and Fe(III)[30,31,42] piano-stool alkynyl complexes (Supporting Information, Table S2); a slight but characteristic lengthening of the Fe−Cp and Fe−P bonds and a shortening of the Fe−C37 bond being observed for the Fe(III) complex **2**[PF$_6$] relative to its Fe(II) parent **2**. Also, in all these compounds, the P−C bonds of the uncoordinated phosphorus atom are close to the average value expected for purely organic triarylphosphines

Rh(I) *trans*-complexes **15** and **16** were readily obtained in nearly quantitative yields and were characterized by NMR (^{1}H and ^{31}P), cyclic voltammetry, land by UV−visible spectroscopy. The crystal structure of **15** could also be solved (Figure 4). Complexation is clearly evidenced by a characteristic shift to higher wavelengths of the metallo-ligand-based MLCT transition, in the 420−450 nm range (Supporting Information), and by an increase in its Fe(II/III) oxidation potential because of the coordination of the Lewis acidic Rh(I) carbonyl fragment to the lone pair of the terminal phosphorus atom. The corresponding complexes with the Fe(III) phosphine ligands **15**[PF$_6$]$_2$ and **16**[PF$_6$]$_2$ were then generated by oxidation of **15**
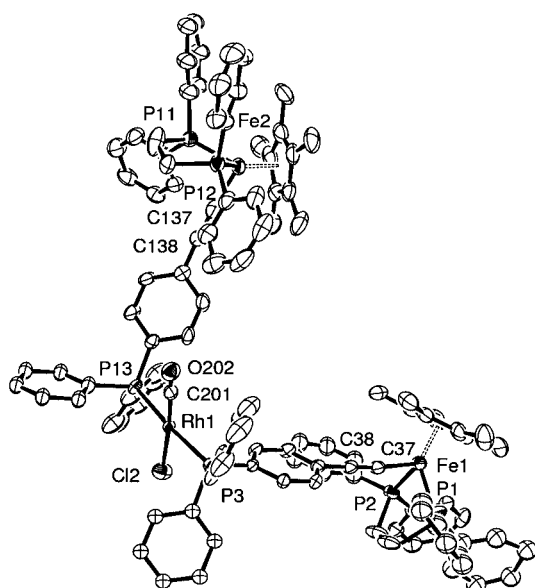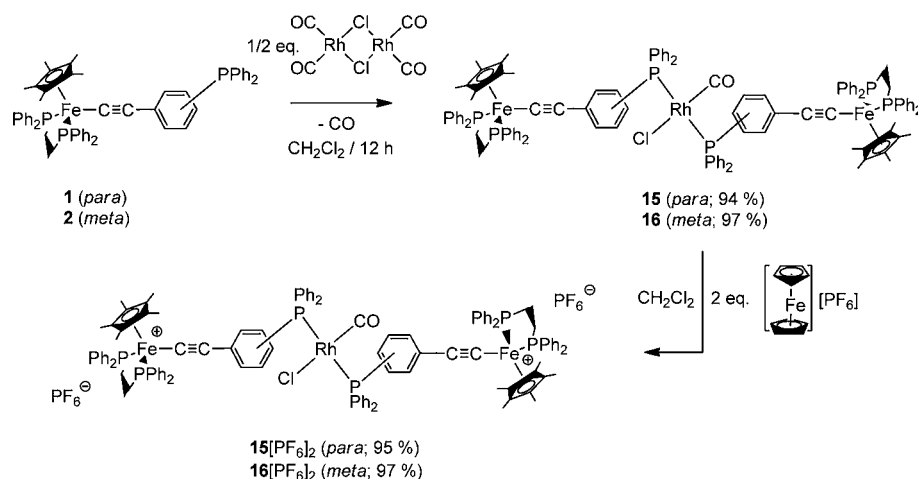
Scheme 4. Synthesis of the Rh(I) Carbonyl Complexes of the Fe(II) and Fe(III) Metallophosphines $1[PF_6]_n$ and $2[PF_6]_n$ ($n = 0$, 1)

Figure 4. ORTEP representations of one of the conformations of the complex **15** present in the asymmetric unit with displacement ellipsoids at the 50% probability level. Selected distances (Å) and angles (deg): Fe1−(Cp*)$_{centroid}$ 1.737, Fe1−P1 2.1821(13), Fe1−P2 2.1735(15), Fe1−C37 1.886(4), C37−C38 1.218(6), C38−C39 1.431(5), Fe2−(Cp*)$_{centroid}$ 1.734, Fe2−P11 2.1884(13), Fe2−P12 2.1671(14), Fe2−C137 1.874(5), C137−C138 1.225(6), C138−C139 1.433(6), Rh1−C201 1.831(6), Rh1−Cl2 2.3683(13), Rh1−P3 2.3143(9), Rh1−P13 2.3170(10), C201−O202 1.069(5), Fe1−C37−C38 174.0(4), C37−C38−C39 179.6(5), Fe2−C137−C138 176.0(4), C137−C138−C139 174.5(5), Rh1−C201-O202 177.9(4), P3−Rh1−C201 92.2, P3−Rh1−Cl1 88.0, C40−C39−Fe1−(Cp*)$_{centroid}$ −144.9, C40−C39−Fe1−(Cp*)$_{centroid}$ −103.2.

Table 3. Evaluation of the Steric (θ_T) and Electronic Parameters for 1−4 and 1−2$[PF_6]$

phosphine	θ_T (deg)[a]	$^1J_{PSe}$ (Hz)[b]	$\nu_{C\equiv O}$ (cm^{-1})[c]	$\Delta\nu_{C\equiv O}$ (cm^{-1})[d]
1	151	747	1975	
1 $[PF_6]$			1979	+4
2	136	752	1977	
2$[PF_6]$	144		1979	+2
3	186	729		
4		744		
PPh$_3$	145[e]	730[f]	1978[g]	
18a	168[h]	746[h]		
18b	175[i]			
19a	155−173[j]	731−3[k]	1970[l]	
19b			1773[m]	

[a]Cone angle determined from available X-ray data (see text). [b] $^1J_{PSe}$ for the corresponding selenophosphine derivatives in C$_6$D$_6$ (±1 Hz). [c]IR in CH$_2$Cl$_2$ solution (±2 cm^{-1}) of the bis(phosphine)chloro(carbonyl) rhodium(I) complex. [d]Fe(II) vs Fe(III) ν_{CO} difference of the corresponding Rh(I) complexes (previous column). [e]See ref 52. [f]See ref 54a. [g]Same value found in CHCl$_3$. [h]See ref 20. [i]See ref 18. [j]See refs 21, 22, 45, and 53. [k]See refs 21 and 54. [l]See refs 45 and 49. [m]See ref 48.

Rh(Ph$_3$P)$_2$(CO)Cl (**17**).[50] The key bond lengths and angles within each metallo-ligand are classic, albeit several phenyl rings appear disordered in the solid state.

■ DISCUSSION

Electronic Structures of the New Metallo-Phosphines 1−4. The Fe(II) metallo-ligands **1−4** have now been fully characterized. In line with the electron-rich nature of the Fe(κ^2-dppe)(η^5-C$_5$Me$_5$) end group(s), the corresponding Fe(III) congeners $1[PF_6]−4[PF_6]_3$ are thermodynamically stable species that can be simply isolated by chemical oxidation (Scheme 3), the oxidation taking place at significantly lower potentials than ferrocene (around −0.12 V vs SCE). Both neutral and oxidized derivatives present diagnostic spectroscopic signatures of Fe(κ^2-dppe)(η^5-C$_5$Me$_5$) alkynyl complexes (Tables 1−2), the latter species corresponding mainly to metal-centered Fe(III) radicals. Comparison of the data obtained for $1[PF_6]_n$ ($n = 0$, 1) with data previously gathered for the model compounds **8-X**$[PF_6]_n$ ($n = 0$, 1)[30,31,34,36] plainly reveals that

(1.837 Å), and a nearly tetrahedral geometry is observed around the phosphorus atom.[57] Comparison between **2** and **2**$[PF_6]$ suggests that these structural features are not significantly altered by oxidation, at least for the mononuclear derivatives.

Regarding the Rh(I) carbonyl complex **15**, the rhodium center exhibits a classic square planar coordination geometry,[45,58] with typical Rh−Cl (2.369 Å), Rh−P (2.314 Å), and Rh−C(O) (1.847 Å) bonds,[59] resembling these observed in

Table 4. Crystal Data, Data Collection, and Refinement Parameters for 1, 2, 2[PF$_6$], 3, and 15

	1	2	2[PF$_6$]	3	15
formula	C$_{56}$H$_{53}$Fe$_1$P$_3$	C$_{56}$H$_{53}$Fe$_1$P$_3$	C$_{56}$H$_{53}$F$_6$Fe$_1$P$_4$	C$_{132}$H$_{129}$Fe$_3$P$_7$	C$_{113}$H$_{106}$Cl$_1$Fe$_2$O$_1$P$_6$Rh$_1$
M_r (g)	874.74	874.74	1019.71	2099.69	1915.86
T (K)	150(2)	100(2)	100(2)	100(2)	150(2)
cryst. syst.	triclinic	monoclinic	monoclinic	trigonal	monoclinic
space group	$P\bar{1}$	$P2_1/n$	Pn	$R\bar{3}$	$P2_1/n$
a /Å	10.9204(5)	12.2780(4)	12.3940(6)	24.5857(9)	11.4178(2)
b /Å	11.1057(4)	21.9742(10)	11.9823(6)	24.5857(0)	28.7416(7)
c /Å	20.2650 (7)	16.8487(7)	16.4380(9)	34.7513(13)	30.8356(7)
α /deg	102.848(2)	90.0	90.0	90.0	90.0
β /deg	94.335(2)	103.994(2)	93.027(3)	90.0	99.0520(10)
γ /deg	107.709(2)	90.0	90.0	120.0	90.0
V/Å^3	2255.33(15)	4410.9(3)	2437.8(2)	18191.4(8)	9993.2(4)
Z	2	4	2	6	
d_{calc} (g cm^{-3})	1.288	1.317	1.389	1.15	1.273
F_{000}	920	1840	1058	6624	3984
number unique refl.	10236	10013	10348	9269	22666
number obs. refl. $[I > 2\sigma(I)]$	8458	7719	9370	7935	14041
R_{int}	0.0350	0.0875	0.0386	0.0397	0.0554
final R	0.038	0.050	0.045	0.044	0.069
R_w	0.094	0.094	0.102	0.109	0.184
R indices (all data)	0.049	0.130	0.050	0.055	0.114
R_w (all data)	0.099	0.072	0.109	0.114	0.201
GOF on F^2 (S_w)	1.079	1.031	1.030	1.074	1.127

PPh$_2$ behaves as a moderately electron-withdrawing group in **1**/ **1**[PF$_6$], but also certainly in the metallo-phosphines **2**/**2**[PF$_6$], in line with the Hammett electron substituent parameters (ESPs) reported for this substituent (σ_p = 0.19 and σ_m = 0.11).[60] This constitutes a significant difference with nitrogen analogues of **1**/**1**[PF$_6$] or **3**/**3**[PF$_6$]$_3$ such as **8-NPh$_2$**/**8-NPh$_2$**[PF$_6$] (X = NPh$_2$) or **14**/**14**[PF$_6$]$_3$ (Scheme 5),[43] for

Scheme 5. Nitrogen Analogues of Fe(II) Alkynyl Complexes 1 and 3

8-NPh$_2$ **14**
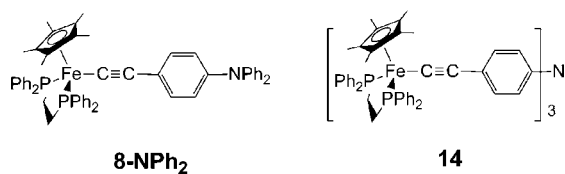
which the pnictogen substituent presents a significant electron-releasing character (σ_p = −0.22, σ_m = 0.00).[60] Such a difference can be primarily ascribed to the difference in group electronegativity between PPh$_2$ and NPh$_2$, also resulting in the different geometry adopted by these substituents in the solid state. Thus, a better overlap between the pnictogen lone pair and the bridging phenyl ring is achieved in **8-NPh$_2$** compared to **1**, as revealed by the X-ray structures of these complexes (C$_{Ph}$−N−C$_{(4-C6H4)}$ angles of about 120 ± 2° in **8-NPh$_2$**,[43] vs C$_{Ph}$−P−C$_{(4-C6H4)}$ angles of about 101 ± 1° in **1**). In line with the available ^{1}H NMR data, the relatively weaker π-donicity of phosphorus compared to nitrogen and its nearly tetrahedral geometry in **3**[PF$_6$]$_3$ make it certainly less prone to convey electronic exchange coupling interactions between unpaired spins in this trication than in **14**[PF$_6$]$_3$.[43]

Steric and Electronic Parameters of the Metallo-Phosphine Ligands. Before further evaluation of these new metallo-phosphines as redox-switchable ligands, we wondered

about their steric and electronic parameters and also about the changes undergone by these features upon oxidation.

The steric parameters of phosphine ligands are often discussed in terms of their Tolman cone-angle values (θ_T).[52] Indeed, compared to alternative measures often used to evaluate the steric requirements of ligands, such as solid angles (Ω) or repulsive energies (E_R), θ_T values can be readily derived and give usually a consistent picture with Ω and E_R.[61] Assuming a correspondence between cone angles in the solid state and in solution, we have derived θ_T values from the available crystallographic data for **1**−**3** and **2**[PF$_6$] (see Supporting Information).[62] A cone angle of 186° was found for the symmetric phosphine **3** (Table 3) while cone angles of 151° and 136° and 144° were similarly derived for the unsymmetrical phosphines **1**, **2**, and **2**[PF$_6$], respectively. Alternatively, an effective θ_T value closer to 164° was found for **1** from the structural data of **15**. Also, based on the θ_T value found for **3** and on that reported for PPh$_3$ (145°), a value of about 159° can be derived for **1** using the procedure of Tolman allowing to estimate the cone of mixed phosphines from the cone angle of the corresponding symmetric phosphines.[52] Remarkably, by reason of the quite folded conformation adopted by this ligand, the θ_T value found for **2** is lower than that of PPh$_3$. Notably, a quite similar conformation is adopted by its oxidized counterpart **2**[PF$_6$], it seems therefore that oxidation will only have a minimum impact on the cone angles of the monometallic derivatives. Because of the possibility of such a "folding", the cone angle of **4** can hardly be estimated from molecular models. In the absence of crystallographic evidence, we would thus tentatively propose that its cone angle is larger than or at least equal to that of **3**.

Various spectroscopic markers have been used to empirically access the electronic parameters of a given phosphine ligand. One way is to use phosphorus−selenium coupling constants ($^1J_{PSe}$) that can be considered as a marker of the s character of the lone pair.[54,63] Thus, the smaller the coupling is, the more

nucleophilic (basic) the phosphine is and the more electron-releasing the peripheral substituents on the aromatic ring must be. In parallel to this work, we have therefore synthesized the corresponding selenium derivatives and measured their $^1J_{PSe}$ values (Table 3). Based on these, the following order can be proposed for the electron-richness of the phosphine ligand: **3** > **4** $\geq$ **1** > **2**. However, according to the values found, it would also seem that the metallo-phosphines **1−2** and **4** are less electron-rich than PPh$_3$, an observation which stands against the well-known electron-releasing character of the $[Fe(\kappa^2\text{-}dppe)(\eta^5\text{-}C_5Me_5)(C{\equiv}C)]-$ end-group.[55,64] Actually, as will be discussed more thoroughly elsewhere, it appears that the ordering found for the metallo-ligands is basically correct, but that the $^1J_{PSe}$ data obtained for metallo-phosphines cannot be compared to those obtained for purely "organic" phosphines such as PPh$_3$ for instance.

A more classic approach to obtain the electronic parameters of a given phosphine ligand is to look at a CO stretching energy of a carbonyl complex to which the ligand is coordinated; ν_{CO} values being shifted to lower values when the phosphine donicity increases. While $[Ni(CO)_3(PR_3)]$ complexes were initially used for such studies,[52] $[Rh(PR_3)_2(CO)Cl]$ complexes have recently been proposed as an interesting alternative, because of their lower toxicity and increased shift range.[45,48] We have therefore synthesized the latter complexes with the mononuclear ligands **1−2**$[PF_6]_n$ in their two (n = 0, 1) redox states, and measured the ν_{CO} values in dichloromethane solution (Table 3). The previous trend (**1** > **2**) can be retrieved from our data, but the differences between ν_{CO} wave numbers remain within experimental uncertainties, evidencing that the electronic changes between them are poorly sensed at a metal center to which they are coordinated. Regarding the Fe(III) metallo-ligands **1−2**$[PF_6]$, a consistent (but very slight) weakening of the ligand donicity is observed compared to their Fe(II) parents. Obviously, considering the range spanned by the data along with its experimental uncertainty,[45] the ν_{CO} wavenumbers are presently less accurate markers than $^1J_{PSe}$ values to compare Fe(II) metalloligands between themselves when only slight changes in donicity take place.

Comparison of the θ_T, $^1J_{PSe}$ and ν_{CO} determined for **1−4** with the scant data available for the known ferrocenyl phosphines **18a−b** or **19a−b** (Scheme 6 and Table

Scheme 6. Related Ferrocenyl Phosphines[24,65]
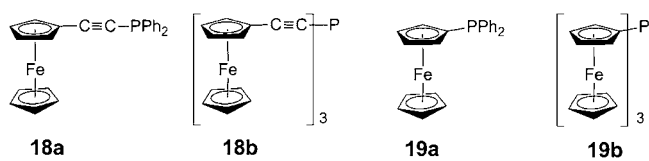
3),[20−22,48,49,53,54] reveals that **1−2** (resp. **3−4**) will present lower cone angles than **18a−19a** (resp. **18b−19b**), but that the donor properties of the para-substituted derivatives **1** and **3** should be comparable to those of **18a−b**, and lower than those of **19a−b**. Note however that from the point of view of redox-switching, **18a−b** or **19a−b** are less attractive ligands than **1−4**. Indeed, oxidation of **18a−b**[20,24] and **19a−b**[21,23e,j,i] takes place at significantly higher redox potentials (usually above 0.5 V vs SCE). Moreover, electrochemical oxidations were reported to be chemically irreversible for **19a**[21,23i,j] or **19b**,[23e] and to yield organometallic radicals of lower kinetic stability at the electrode for **18a−b** than for **1−4**.[20]

CONCLUSIONS

We have reported here the synthesis and characterization of four new Fe(II) triphenylphosphine ligands (**1−4**) functionalized with electron-rich $[Fe(\kappa^2\text{-}dppe)(\eta^5\text{-}C_5Me_5)(C{\equiv}C)]$ substituents at their periphery, along with the evaluation of their electronic and steric parameters (θ_T). Based on these estimates, these new metallo-phosphine ligands appear to be only slightly more electron-donating than PPh$_3$. Among these, the *para* derivatives appear comparable to related ferrocenyl-thynyl-phosphine ligands, but less electron-donating than ferrocenylphosphine analogues. On steric grounds, they certainly compare to their ferrocenyl or ferrocenylethynyl analogues, and are clearly bulkier than PPh$_3$, except perhaps for **2**. An interesting advantage over the ferrocenyl-based ligands is that **1−4** are oxidized at significantly lower potentials and give rise to remarkably more stable cationic species, a feature certainly in part attributable to the largely metal-centered nature of the electronic vacancy generated by oxidation.[32]

Regarding their charge distribution, all the Fe(II) metallo-phosphines present a dipolar or multipolar structure characterized by electron-rich site(s) located on the iron center(s) and an electron-poorer site located on the terminal/central phosphorus atom. This structure is significantly altered by oxidation; however, the electronic changes induced by oxidation appear to be only moderately sensed at the metal center to which these metallo-ligands are coordinated. Actually, these changes resemble those that would be induced by replacing the electron-releasing Fe(II) organometallic end group(s) on the phenyl ring(s) by a very weakly electron-withdrawing substituent. While these purely inductive/meso-meric changes induced on the phosphorus atom by oxidation of the $[Fe(\kappa^2\text{-}dppe)(\eta^5\text{-}C_5Me_5)(C{\equiv}C)]$ substituent(s) may seem too weak to strongly influence the reactivity of a remote metal center, it should however be remembered that they are accompanied by the creation of electronic vacancies localized on the substituents of the phosphine ligand, along with the creation of positive charge(s). Depending on the actual nature of the metal center coordinated to it and of the surrounding medium, both of these features might also be able to influence profoundly its reactivity, either by intramolecular electron-transfer or by purely through-space electrostatic interactions. Moreover, we would like to stress here that redox-switchable metalloligands such as **1−4** might lead to interesting applications in fields more related to material sciences, and different from catalysis, especially those for which a large electronic interaction between the redox-active iron center and the terminal phosphine group that binds to a given metal center is less crucial in the ground state.[3,66]

EXPERIMENTAL SECTION

General Procedures. All reactions and workup procedures were carried out under dry, high purity argon using standard Schlenk techniques.[67] All solvents were freshly distilled and purged with argon before use. Infrared spectra were obtained on a Bruker IFS28 FT-IR spectrometer (400−4000 cm^{-1}). Raman spectra of the solid samples were obtained by diffuse scattering on the same apparatus and recorded in the 100−3300 cm^{-1} range (Stokes emission) with a laser excitation source at 1064 nm (25 mW) and a quartz separator with a FRA 106 detector. NMR spectra were acquired at 298 K on a Bruker DPX200 and Bruker AV300P (300 MHz) or on a Bruker AVANCE 500, equipped with a 5 mm broadband observe probe and a z-gradient coil. Chemical shifts are given in parts per million (ppm) and referenced to the residual nondeuterated solvent signal[68] for ^1H and ^{13}C and external H$_3$PO$_4$ (0.0 ppm) for ^{31}P NMR spectra. Experimental

details regarding measurements on paramagnetic Fe(III) complexes can be found in previous contributions.[5,30,42] Cyclic voltammograms were recorded in dry CH_2Cl_2 solutions (containing 0.10 M [$^nBu_4N$][PF_6], purged with argon and maintained under argon atmosphere) using a EG&G-PAR model 263 potentiostat/galvanostat. The working electrode was a Pt disk, the counter electrode a Pt wire and the reference electrode a saturated calomel electrode. The $FeCp_2^{0/1+}$ couple ($E_{1/2}$: 0.46 V, ΔEp = 0.08 V; I_p^a/I_p^c = 1) was used as an internal calibrant for the potential measurements.[69] Near-IR and UV−visible spectra were recorded as CH_2Cl_2 solutions, using a 1 cm long quartz cell on a Cary 5000 spectrometer. Electron paramagnetic resonance (EPR) spectra were recorded on a Bruker EMX-8/2.7 (X-band) spectrometer, at 77 K (liquid nitrogen). Elemental analysis and high resolution mass spectra (ESI on Micromass MS/MS ZABSpec TOF spectrometer) were performed at the "Centre Regional de Mesures Physiques de l'Ouest" (CRMPO), Université de Rennes 1.

The complex [Fe(κ^2-dppe)(η^5-C$_5$Me$_5$)Cl] (13),[70] the organic phosphines 9−12,[33] and [(η^5-C$_5$H$_5$)$_2$Fe][PF$_6$][69] were prepared as described in the literature. Other chemicals were purchased from commercial suppliers and used as received. Whenever needed, silica (Merck Kieselgel 60; 0.063−0.200 mm) was deactivated by stirring in a mixture of n-hexane and triethylamine (10:1), then packed in a column and washed with pure CH_2Cl_2. The plug of silica was dried in vacuo for 2 h and used under argon.

Synthesis of the Mononuclear Fe(II) Metallophosphines (1− 2). In a Schlenk tube, the complex [Fe(κ^2-dppe)(η^5-C$_5$Me$_5$)Cl] (13; 625 mg, 1 mmol), KPF$_6$ (221 mg, 1.2 mmol) and 9/10 (344 mg, 1.2 mmol) were dissolved in tetrahydrofuran (THF, 15 mL) and MeOH (15 mL) and stirred 12 h at 25 °C. After removal of the solvents, the dark brown residue was extracted with dichloromethane and concentrated in vacuo (ca. 5 mL). Precipitation by addition of n-pentane and filtration gave the corresponding vinylidene complexes (vin-1[PF$_6$]/vin-2[PF$_6$]), isolated as brown powders.

[Fe(κ^2-dppe)(η^5-C$_5$Me$_5$)═C═CH(p-C$_6$H$_4$PPh$_2$)][PF$_6$] (vin-1[PF$_6$]). Yield: 96%. ^{31}P{^{1}H} NMR (121 MHz, CDCl$_3$): δ = 86.5 (s, 2P, P_{dppe}), −5.2 (s, 1P, PPh$_2$), −144.3 (sept, 1P, J_{PF} = 713 Hz, PF$_6$). ^{1}H NMR (300 MHz, CDCl$_3$): δ = 7.60−7.11 (m, 30H, H_{aryl}), 6.68 (m, 2H, H_{aryl}), 6.22 (m, 2H, H_{aryl}), 5.10 (m, 1H, $H_{vinylidene}$), 3.05 (m, 2H, $CH_{2/dppe}$), 2.48 (m, 2H, $CH_{2/dppe}$), 1.57 (s, 15H, C$_5$(CH$_3$)$_5$).

[Fe(κ^2-dppe)(η^5-C$_5$Me$_5$)═C═CH(m-C$_6$H$_4$PPh$_2$)][PF$_6$] (vin-2[PF$_6$]). Yield: 93%. ^{31}P{^{1}H} NMR (121 MHz, CDCl$_3$): δ = 87.3 (s, 2P, P_{dppe}), −5.2 (s, 1P, PPh$_2$), −144.3 (sept, 1P, J_{PF} = 713 Hz, PF$_6$). ^{1}H NMR (300 MHz, CDCl$_3$): δ = 7.57−7.13 (m, 30H, H_{aryl}), 6.92−6.80 (m, 2H, H_{aryl}), 6.50 (m, 1H, H_{aryl}), 6.30 (m, 1H, H_{aryl}), 4.98 (m, 1H, $H_{vinylidene}$), 3.02 (m, 2H, $CH_{2/dppe}$), 2.48 (m, 2H, $CH_{2/dppe}$), 1.50 (s, 15H, C$_5$(CH$_3$)$_5$).

These vinylidene salts (vin-1[PF$_6$]/vin-2[PF$_6$]) were stirred for 1h in THF in the presence of excess DBU (0.22 mL, 1.5 mmol). The solvent was then removed in vacuo, and the residue was purified by column chromatography under argon atmosphere (deactivated silica gel, toluene). Removal of toluene in vacuo and washing of the resulting solid with n-pentane afforded the desired alkynyl complexes as orange powders.

Fe(κ^2-dppe)(η^5-C$_5$Me$_5$)C≡C(p-C$_6$H$_4$PPh$_2$) (1). Total yield: 72%. X-ray quality crystals could be grown by slow diffusion of either n-pentane or methanol in a dichloromethane solution of the complex. Anal. Calc for C$_{56}$H$_{53}$P$_3$Fe: C, 76.89; H, 6.11; Found: C, 76.62; H, 6.27. HRMS: calc 874.2709 [M$^{+\cdot}$], found 874.2711. Raman (neat, cm^{-1}): ν = 2054 (vs, C≡C), 2019 (w, C≡C). ^{1}H NMR (300 MHz, C$_6$D$_6$): δ = 7.98−7.93 (m, 4H, H_{aryl}), 7.47−7.02 (m, 30H, H_{aryl}), 2.58 (m, 2H, $CH_{2/dppe}$), 1.80 (m, 2H, $CH_{2/dppe}$), 1.50 (s, 15H, C$_5$(CH$_3$)$_5$). UV−vis (CH$_2$Cl$_2$): λ_{max}/nm [$\varepsilon/10^3$ M^{-1}·cm^{-1}] = 273 (sh) [45.9], 328 [15.2], 387 [18.0], 424 (sh) [14.8].

Fe(κ^2-dppe)(η^5-C$_5$Me$_5$)C≡C(m-C$_6$H$_4$PPh$_2$) (2). Total yield: 73%. X-ray quality crystals were grown from slow diffusion of n-pentane in a chloroform solution of the complex. HRMS: calc 874.2709 [M$^{+\cdot}$], found 874.2705. Raman (neat, cm^{-1}): ν = 2072 (vw, C≡C), 2063 (w, C≡C), 2036 (vs, C≡C). ^{1}H NMR (300 MHz, C$_6$D$_6$): δ = 7.97− 7.92 (m, 4H, H_{aryl}), 7.48−7.42 (m, 4H, H_{aryl}), 7.30−7.04 (m, 26H, H_{aryl}), 2.53 (m, 2H, $CH_{2/dppe}$), 1.77 (m, 2H, $CH_{2/dppe}$), 1.48 (s, 15H,

C$_5$(CH$_3$)$_5$). UV−vis (CH$_2$Cl$_2$): λ_{max}/nm [$\varepsilon/10^3$ M^{-1}·cm^{-1}] = 261 (sh) [49.4], 328 [12.8], 365 [13.2], 398 (sh) [11.1].

Synthesis of the Trinuclear Fe(II) Metallophosphines (3−4). In a Schlenk tube, the complex [Fe(κ^2-dppe)(η^5-C$_5$Me$_5$)Cl] (13; 656 mg, 1.05 mmol), KPF$_6$ (193 mg, 1.05 mmol) and 11/12 (100 mg, 0.3 mmol) were dissolved in THF (15 mL) and MeOH (15 mL) and stirred for 2 days at 40 °C. After removal of the solvents, the dark brown residue was extracted with dichloromethane and concentrated in vacuo (ca. 5 mL). Precipitation by addition of n-pentane and filtration gave the corresponding tris-vinylidene complexes (vin-3[PF$_6$]$_3$/vin-4[PF$_6$]$_3$), isolated as brown powders.

[{Fe(κ^2-dppe)(η^5-C$_5$Me$_5$)═C═CH(p-C$_6$H$_4$)}$_3$P][PF$_6$]$_3$ (vin-3[PF$_6$]$_3$). Yield: 89%. ^{31}P{^{1}H} NMR (81 MHz, CDCl$_3$): δ = 87.8 (s, 6P, P_{dppe}), −4.2 (broad s, 1P, PAr$_3$), −143.1 (sept, 3P, J_{PF} = 713 Hz, PF$_6$). ^{1}H NMR (200 MHz, CDCl$_3$): δ = 7.64−7.19 (m, 60H, H_{aryl}), 6.83 (m, 6H, H_{aryl}), 6.38 (m, 6H, H_{aryl}), 5.11 (broad s, 3H, $H_{vinylidene}$), 3.14 (m, 6H, $CH_{2/dppe}$), 2.55 (m, 6H, $CH_{2/dppe}$), 1.62 (s, 45H, C$_5$(CH$_3$)$_5$).

[{Fe(κ^2-dppe)(η^5-C$_5$Me$_5$)═C═CH(m-C$_6$H$_4$)}$_3$P][PF$_6$]$_3$ (vin-4[PF$_6$]$_3$). Yield: 85%. ^{31}P{^{1}H} NMR (81 MHz, CDCl$_3$): δ = 88.2 (s, 6P, P_{dppe}), −143.1 (sept, 3P, J_{PF} = 713 Hz, PF$_6$), the signal corresponding to the (C$_6$H$_4$)$_3$P was not detected (presumably too broad). ^{1}H NMR (200 MHz, CDCl$_3$): δ = 7.58−6.89 (m, 72H, H_{aryl}), 4.93 (broad s, 3H, $H_{vinylidene}$), 2.92 (m, 6H, $CH_{2/dppe}$), 2.39 (m, 6H, $CH_{2/dppe}$), 1.52 (s, 45H, C$_5$(CH$_3$)$_5$).

These tris-vinylidene salts (vin-3[PF$_6$]$_3$/vin-4[PF$_6$]$_3$) were stirred for 1 h in THF in the presence of excess DBU (0.22 mL, 1.5 mmol). The solvent was then removed in vacuo, and the residue was purified by column chromatography under argon atmosphere (deactivated silica gel, toluene). Removal of toluene in vacuo and washing of the resulting solid with n-pentane afforded the tris-alkynyl complexes as orange powders.

[Fe(κ^2-dppe)(η^5-C$_5$Me$_5$)C≡C(p-C$_6$H$_4$)]$_3$P (3). Total yield: 71%. X-ray quality crystals were grown from slow diffusion of Et$_2$O in a dichloromethane solution of the complex. Anal. Calc for C$_{132}$H$_{129}$P$_7$Fe$_3$: C, 75.50; H, 6.19; Found: C, 75.66; H, 6.42. HRMS: calc: 2098.63059 [M$^{+\cdot}$], found: 2098.6357. ^{1}H NMR (300 MHz, C$_6$D$_6$): δ = 7.98 (m, 12H, H_{aryl}), 7.49−7.44 (m, 6H, H_{aryl}), 7.14−6.99 (m, 54H, H_{aryl}), 2.62 (m, 6H, $CH_{2/dppe}$), 1.83 (m, 6H, $CH_{2/dppe}$), 1.52 (s, 45H, C$_5$(CH$_3$)$_5$). UV−vis (CH$_2$Cl$_2$): λ_{max}/nm [$\varepsilon/10^3$ M^{-1}·cm^{-1}] = 265 (sh) [80.8], 328 (sh) [29.3], 392 [37.4], 424 (sh) [32.9].

[Fe(κ^2-dppe)(η^5-C$_5$Me$_5$)C≡C(m-C$_6$H$_4$)]$_3$P (4). Total yield 74%. Anal. Calc for C$_{132}$H$_{129}$P$_7$Fe$_3$: C, 75.50; H, 6.19; Found: C, 75.55; H, 6.14. HRMS: calc: 2098.6306 [M$^{+\cdot}$], found: 2098.6315. ^{1}H NMR (300 MHz, C$_6$D$_6$): δ = 8.01−7.97 (m, 12H, H_{aryl}), 7.53 (d, $^3J_{HH}$ = 9 Hz, 3H, H_{aryl}), 7.33−7.02 (m, 57H, H_{aryl}), 2.57 (m, 6H, $CH_{2/dppe}$), 1.78 (m, 6H, $CH_{2/dppe}$), 1.51 (s, 45H, C$_5$(CH$_3$)$_5$). UV−vis (CH$_2$Cl$_2$): λ_{max}/nm [$\varepsilon/10^3$ M^{-1}·cm^{-1}] = 261 (sh) [51.8], 306 (sh) [18.2], 365 [21.5], 404 (sh) [16.5].

Synthesis of the Mononuclear Fe(III) Metallophosphines (1[PF$_6$]−2[PF$_6$]). In a Schlenk tube, the Fe(II) complexes 1/2 (219 mg, 0.25 mmol) and [FcH][PF$_6$] (83 mg, 0.25 mmol) were dissolved in THF (15 mL) and stirred for 1 h at room temperature. After removal of the solvent, the residue was dissolved in dichloromethane (5 mL) and precipitated by addition of n-pentane. Filtration and drying in vacuo gave the corresponding Fe(III) complexes 1[PF$_6$]/ 2[PF$_6$] as black powders.

[Fe(κ^2-dppe)(η^5-C$_5$Me$_5$)C≡C(p-C$_6$H$_4$PPh$_2$)][PF$_6$] (1[PF$_6$]). Yield: 94%. ^{31}P{^{1}H} NMR (121 MHz, CD$_2$Cl$_2$): δ = 252.8 (broad s, ArPPh$_2$), P_{dppe} and PF$_6^-$ not detected. ^{1}H NMR (500 MHz, CD$_2$Cl$_2$): δ = 28.9 (broad s, H_2), 8.0 (s, H_{Ph}), 7.9 (s, $H_{Ph/dppe}$), 7.5−7.3 (s, H_3+H_5), 6.8 (s, $H_{Ph/dppe}$), 6.6 (s, $CH_{2/dppe}$), 6.2 (s, $H_{Ph/dppe}$), 3.7 (s, $H_{Ph/dppe}$), 1.7 (s, $H_{Ph/dppe}$), −2.7 (broad s, $CH_{2/dppe}$), −10.4 (broad s, C$_5$(CH$_3$)$_5$), −39.0 (very broad s, H_1) [See Chart 1 for labeling]. UV−vis (CH$_2$Cl$_2$): λ_{max}/nm [$\varepsilon/10^3$ M^{-1}·cm^{-1}] = 261 [37.2], 320 [20.9], 495 (sh) [3.2], 568 [1.8], 653 [1.8].

[Fe(κ^2-dppe)(η^5-C$_5$Me$_5$)C≡C(m-C$_6$H$_4$PPh$_2$)][PF$_6$] (2[PF$_6$]). Yield 96%. X-ray quality crystals were grown from slow diffusion of n-pentane in a dichloromethane solution of the complex. ^{31}P{^{1}H} NMR (121 MHz, CD$_2$Cl$_2$): δ = −29.2 (s, ArPPh$_2$), P_{dppe} and PF$_6^-$ not detected. ^{1}H NMR (500 MHz, CD$_2$Cl$_2$): δ = 29.1 (broad s, 1H, H_2),

7.9 (s, $H_{Ph/dppe}$), 7.6−7.5 (2s, H_3+H_5), 7.3 (s, H_4), 6.7 (s, $H_{Ph/dppe}$), 6.7 (broad s, $CH_{2/dppe}$), 6.2 (s, $H_{Ph/dppe}$), 3.6 (s, $H_{Ph/dppe}$), 1.5 (s, $H_{Ph/dppe}$), −2.8 (broad s, $CH_{2/dppe}$), −10.4 (broad s, $C_5(CH_3)_5$), −41.5 (very broad s, 3H, H_1+ $H_{1'}$+$H_{1''}$) [See Chart 1 for labeling]. UV−vis (CH_2Cl_2) λ_{max}/nm [ε/10^3 M^{-1}·cm^{-1}] = 259 [51.1], 281 (sh) [44.1], 306 (sh) [25.5], 393 (sh) [3.9], 583 [2.8], 670 [3.9].

Synthesis of the Trinuclear Fe(III) Metallophosphines (3-[PF$_6$]$_3$−4[PF$_6$]$_3$). In a Schlenk tube, Fe(II) complexes **3**/**4** (210 mg, 0.1 mmol) and [FcH][PF$_6$] (99 mg, 0.3 mmol) were dissolved in THF (15 mL) and stirred for 1 h at room temperature. After removal of the solvent, the residue was dissolved in dichloromethane (5 mL) and precipitated by addition of *n*-pentane. Filtration and drying in vacuo gave the corresponding Fe(III) complexes **3**[PF$_6$]$_3$/**4**[PF$_6$]$_3$ as black powders.

[{Fe(κ^2-dppe)(η^5-C_5Me_5)C≡C(p-C_6H_4)}$_3$P][PF$_6$]$_3$ (**3[PF$_6$]$_3$**). Yield: 91%. ^{31}P{^{1}H} NMR (202 MHz, CD$_2$Cl): δ = 520.6 (broad s, ArPPh$_2$), P_{dppe} and PF$_6^-$ not detected. ^{1}H NMR (500 MHz, CD$_2$Cl$_2$): δ = 28.4 (broad s, H_2), 7.9 (s, $H_{Ph/ArPPh_2}$), 6.9 (s, $H_{Ph/dppe}$), 6.4 (broad s, $CH_{2/dppe}$), 6.2 (s, $H_{Ph/dppe}$), 3.6 (s, $H_{Ph/dppe}$), 1.6 (s, $H_{Ph/dppe}$), −2.7 (broad s, $CH_{2/dppe}$), −10.4 (broad s, $C_5(CH_3)_5$), −36.6 (very broad s, H_1) [See Chart 1 for labeling]. UV−vis (CH_2Cl_2): λ_{max}/nm [ε/10^3 M^{-1}·cm^{-1}] = 267 [142.61], 325 [95.2], 403 (sh) [21.2], 587 [8.2], 695 [11.9].

[{Fe(κ^2-dppe)(η^5-C_5Me_5)C≡C(m-C_6H_4)}$_3$P][PF$_6$]$_3$ (**4[PF$_6$]$_3$**). Yield: 89%. ^{31}P{^{1}H} NMR (202 MHz, CD$_2$Cl$_2$): δ = −40.9 (s, ArPPh$_2$), P_{dppe} and PF$_6^-$ not detected. ^{1}H NMR (500 MHz, CD$_2$Cl$_2$): δ = 27.3 (broad s, 1H, H_2), 7.9 (s, $H_{Ph/dppe}$), 6.8 (s, $H_{Ph/dppe}$), 6.4 (broad s, $CH_{2/dppe}$), 6.1 (s, $H_{Ph/dppe}$), 3.7 (s, $H_{Ph/dppe}$), 1.6 (s, $H_{Ph/dppe}$), −2.8 (broad s, $CH_{2/dppe}$), −10.4 (broad s, $C_5(CH_3)_5$), −33.7 and −35.4 (very broad s, 1H and 2H, H_1+$H_{1'}$+$H_{1'}$) [See Chart 1 for labeling]. UV−vis (CH_2Cl_2): λ_{max}/nm [ε/10^3 M^{-1}·cm^{-1}] = 258 [114.3], 281 (sh) [44.1], 310 (sh) [65.5], 390 (sh) [11.1], 574 [7.3], 662 [8.4].

Synthesis of Rh(I) Carbonyl Complexes of the Fe(II) Metallophosphines. In a dry Schlenk tube, [Rh(CO)$_2$Cl]$_2$ (21.5 mg, 55.3 μmol) and the corresponding phosphines **1** or **2** (194 mg, 221.2 μmol) were dissolved in dichloromethane (5 mL) and stirred overnight at room temperature. Addition of either *n*-pentane or methanol and filtration gave the desired Rh(I) carbonyl complexes as orange powders.

[Fe(κ^2-dppe)(η^5-C_5Me_5)C≡C(p-C_6H_4PPh$_2$)]$_2$Rh(CO)Cl (**15**). Yield: 94%. X-ray quality crystals were grown from slow diffusion of methanol in a dichloromethane solution of the complex. HRMS: calc: 1914.4106 [M$^{+\cdot}$], found: 1914.4133. IR (KBr, cm^{-1}): ν = 1969 (s, CO). Raman (neat, cm^{-1}): ν = 2044 (w, C≡C). ^{1}H NMR (300 MHz, C$_6$D$_6$): δ = 8.02−7.89 (m, 20H, H_{aryl}), 7.30−7.02 (m, 48H, H_{aryl}), 2.57 (m, 4H, CH_2 dppe), 1.79 (m, 4H, CH_2 dppe), 1.50 (s, 30H, $C_5(CH_3)_5$). UV−vis (CH_2Cl_2): λ_{max}/nm [ε/10^3 M^{-1}·cm^{-1}] = 274 [60.0], 378 (sh) [28.7], 422 [34.3].

[Fe(κ^2-dppe)(η^5-C_5Me_5)C≡C(m-C_6H_4PPh$_2$)]$_2$Rh(CO)Cl (**16**). Yield: 97%. HRMS: calc: 1914.4106 [M$^{+\cdot}$], found: 1914.4106. IR (KBr, cm^{-1}): ν = 1973 (s, CO). Raman (neat, cm^{-1}): ν = 2039 (m, C≡C). ^{1}H NMR (300 MHz, C$_6$D$_6$): δ = 8.06−7.88 (m, 16H, H_{aryl}), 7.30−7.02 (m, 52H, H_{aryl}), 2.52 (m, 4H, CH_2 dppe), 1.76 (m, 4H, CH_2 dppe), 1.46 (s, 30H, $C_5(CH_3)_5$). UV−vis (CH_2Cl_2): λ_{max}/nm [ε/10^3 M^{-1}·cm^{-1}] = 286 (sh) [41.5], 365 [25.5], 409 (sh) [18.6].

Synthesis of Rh(I) Carbonyl Complexes of the Fe(III) Metallophosphines. In a dry Schlenk tube, Rh(I) complexes **15** or **16** (200 mg, 0.1 mmol) and [FcH][PF6] (70 mg, 0.2 mmol) were dissolved in dichloromethane (10 mL) and stirred for 1 h at room temperature. Addition of n-pentane and filtration gave the Fe(III) complexes **15**[PF$_6$]$_2$/**16**[PF$_6$]$_2$ as black solids.

[{Fe(κ^2-dppe)(η^5-C_5Me_5)C≡C(p-C_6H_4PPh$_2$)}$_2$Rh(CO)Cl][PF$_6$]$_2$ (**15-[PF$_6$]$_2$**). Yield: 95%. IR (KBr, ν in cm^{-1}): 1973 (s, CO). Raman (neat, cm^{-1}): ν = 2007 (m, C≡C). ^{31}P{^{1}H} NMR (121 MHz, CD$_2$Cl$_2$): δ = −17.8 (broad s, ArPPh$_2$), P_{dppe} and PF$_6^-$ not detected. ^{1}H NMR (300 MHz, CD$_2$Cl$_2$): δ = 28.4 (broad s, H_2), 7.8 (s, H_{Ph} + $H_{Ph/dppe}$), 7.6−7.5 (s, H_{Ph}), 6.9 (s, $H_{Ph/dppe}$), 6.3 (very broad s, $CH_{2/dppe}$), 6.2 (s, $H_{Ph/dppe}$), 3.6 (s, $H_{Ph/dppe}$), 1.5 (s, $H_{Ph/dppe}$), −2.7 (broad s, $CH_{2/dppe}$), −10.6 (broad s, $C_5(CH_3)_5$), −33.9 (very broad s, H_1) [See Chart 1 for labeling]. UV−vis (CH_2Cl_2): λ_{max}/nm [ε/10^3

M^{-1}·cm^{-1}] = 262 [87.6], 324 [53.6], 396 (sh) [12.0], 582 [5.0], 678 [6.4].

[{Fe(κ^2-dppe)(η^5-C_5Me_5)C≡C(m-C_6H_4PPh$_2$)}$_2$Rh(CO)Cl][PF$_6$]$_2$ (**16-[PF$_6$]$_2$**). Yield: 97%. IR (KBr, cm^{-1}): ν = 1973 (s, CO). Raman (neat, cm^{-1}): ν = 2010 (w, C≡C). ^{31}P{^{1}H} NMR (121 MHz, CD$_2$Cl$_2$): δ = 63.8 (d, ^{1}J$_{P-Rh}$ ∼ 124 Hz, ArPPh$_2$), P_{dppe} and PF$_6^-$ not detected. ^{1}H NMR (300 MHz, CD$_2$Cl$_2$): δ = 27.9 (broad s, H_2), 8.0 (s, H_{Ph}), 7.9 (s, $H_{Ph/dppe}$), 7.6 (s, H_{Ph}), 7.4 (s, H_{Ph}), 6.7 (s, $H_{Ph/dppe}$), 6.5 (very broad s, $CH_{2/dppe}$), 6.1 (s, $H_{Ph/dppe}$), 3.8 (s, $H_{Ph/dppe}$), 1.8 (s, $H_{Ph/dppe}$), −2.6 (broad s, $CH_{2/dppe}$), −9.9 (broad s, $C_5(CH_3)_5$), −38.1 (very broad s, 3H, H_1+$H_{1'}$+$H_{1''}$) [See Chart 1 for labeling]. UV−vis (CH_2Cl_2) λ_{max}/nm [ε/10^3 M^{-1}·cm^{-1}] = 254 [88.3], 286 (sh) [65.7], 307 (sh) [47.3], 349 (sh) [15.6], 575 [4.0], 663 [5.0].

Crystallography. Data collection of the various crystals was performed on a KappaCCD diffractometer, at 120(2) K, with graphite monochromatized MoK$_\alpha$ radiation (λ = 0.71073 Å). The structure was solved by direct methods using the SIR97 program,[71] and then refined with full-matrix least-squares methods based on F^2 (SHELX-97)[72] with the aid of the WINGX[73] program. For **3** and **15**, the contribution of the disordered and unidentified residual electronic densities to the calculated structure factors was estimated following the BYPASS algorithm,[74] implemented as the SQUEEZE option in PLATON.[75] A new data set, free of solvent contribution, was then used in the final refinement. The complete structures were refined with SHELXL97[72] by the full-matrix least-squares technique. All non-hydrogen atoms were refined with anisotropic atomic displacement parameters. H atoms were finally included in their calculated positions. A final refinement on F^2 converged to the ωR(F^2) values indicated (Table 4). Bruker AXS BV diffractometer atomic scattering factors were taken from the literature.[76]

Crystallographic Derivation of Cone Angles. Cif files for **1**, **2**, **3**, and **2**[PF$_6$] containing a dummy atom at 2.28 Å along a line linking the barycenter of the three *ipso* carbon atoms and the phosphorus atom. Based on these cif files, the cone angles at the phosphorus can be derived following the procedure proposed by Mingos et al. and considering a van der Waals radius of 1.09 Å for hydrogen.[62]

■ ASSOCIATED CONTENT

Ⓢ Supporting Information

UV−vis spectra and cyclic voltammograms for all compounds. ESR spectra for all Fe(III) compounds. ^{1}H NMR spectra, assignment, and temperature dependence of selected protons of **1**−**2**[PF$_6$] and **3**−**4**[PF$_6$]$_3$. Crystallographic (CIF) file for **1**, **2**, **2**[PF$_6$], **3**, and **15**. This material is available free of charge via the Internet at http://pubs.acs.org. Final atomic positional coordinates, with estimated standard deviations, bond lengths and angles, and anisotropic thermal parameters have been deposited at the Cambridge Crystallographic Data Centre and were allocated the deposition numbers CCDC 925017, CCDC 755887, CCDC 925015, CCDC 925016, and CCDC 925018, respectively.

■ AUTHOR INFORMATION

Corresponding Author

*E-mail: frederic.paul@univ-rennes1.fr.

Notes

The authors declare no competing financial interest.

■ ACKNOWLEDGMENTS

■ REFERENCES

(1) (a) Balzani, V.; de Silva, A. P. *Electron Transfer in Chemistry*; Wiley-VCH: Weinheim, Germany, 2000; Vol. 5; (b) Norgaard, K.; Bjornholm, T. *Chem. Commun.* **2005**, 1812−1823. (c) Gianneschi, N. C.; Masar, M. S., III; Mirkin, C. A. *Acc. Chem. Res.* **2005**, *38*, 825−837. (d) Lehn, J.-M. *Angew. Chem., Int. Ed.* **1990**, *29*, 1304−1319. (e) Lehn, J.-M. *Supramolecular Chemistry - Concepts and Perspectives*; VCH Publishers: Weinheim, Germany, 1995.

(2) (a) Lin, Y.-C.; Chen, W.-T.; Tai, J.; Su, D.; Huang, S.-Y.; Lin, I.; Lin, J.-L.; Lee, M. M.; Chiou, M. F.; Liu, Y.-H.; Kwan, K.-S.; Chen, Y.-J.; Chen, H.-Y. *Inorg. Chem.* **2009**, *48*, 1857−1872. (b) Packheiser, R.; Ecorchard, P.; Walfort, B.; Lang, H. *J. Organomet. Chem.* **2008**, *693*, 933−946. (c) Coe, B. J. *Acc. Chem. Res.* **2006**, *39*, 383−393. (d) Qi, H.; Sharma, S.; Li, Z.; Snider, G. L.; Orlov, A. O.; Lent, C. S.; Fehlner, T. P. *J. Am. Chem. Soc.* **2003**, *125*, 15250−15259. (e) Jiao, J.; Long, G. J.; Rebbouh, L.; Grandjean, F.; Beatty, A. M.; Fehlner, T. P. *J. Am. Chem. Soc.* **2005**, *127*, 17819−17831. (f) Perruchas, S.; Avarvari, N.; Rondeau, D.; Levillain, E.; Batail, P. *Inorg. Chem.* **2005**, *44*, 3459−3465. (g) Kühn, F. E.; Zuo, J.-L.; de Biani, F. F.; Santos, A. M.; Zhang, Y.; Zhao, J.; Sandulache, A.; Herdtweck, E. *New J. Chem.* **2004**, *28*, 43−51. (h) Engratkul, C.; Schoemaker, W. J.; Grzybowski, J. J.; Guzei, I.; Rheingold, A. *Inorg. Chem.* **2000**, *39*, 5161−5163. (i) Ziessel, R. *Synthesis* **1999**, 1839−1865.

(3) Ge, Q.; Corkery, T. C.; Humphrey, M. G.; Samoc, M.; Hor, T. S. A. *Dalton Trans.* **2008**, 2929−2936.

(4) (a) Malvolti, F.; Trujillo, A. M.; Cador, O.; Gendron, F.; Costuas, K.; Halet, J.-F.; Bondon, A.; Toupet, L.; Molard, Y.; Cordier, S.; Paul, F. *Inorg. Chim. Acta* **2011**, *374*, 288−301. (b) Paul, F.; Goeb, S.; Justaud, F.; Argouarch, G.; Toupet, L.; Ziessel, R. F.; Lapinte, C. *Inorg. Chem.* **2007**, *46*, 9036−9038.

(5) Paul, F.; Malvolti, F.; da Costa, G.; Stang, S. L.; Justaud, F.; Argouarch, G.; Bondon, A.; Sinbandhit, S.; Costuas, K.; Toupet, L.; Lapinte, C. *Organometallics* **2010**, *29*, 2491−2502.

(6) (a) Justaud, F.; Argouarch, G.; Gazalah, S. I.; Toupet, L.; Paul, F.; Lapinte, C. *Organometallics* **2008**, *27*, 4260−4264. (b) Ibn Ghazala, S.; Gauthier, N.; Paul, F.; Toupet, L.; Lapinte, C. *Organometallics* **2007**, *26*, 2308−2317.

(7) Le Stang, S.; Paul, F.; Lapinte, C. *Inorg. Chim. Acta* **1999**, *291*, 403−425.

(8) Justaud, F.; Roisnel, T.; Lapinte, C. *New J. Chem.* **2011**, *35*, 2219−2226.

(9) For selected examples using other redox-active organometallics than ferrocene to access molecular devices, see for instance: (a) Cordiner, R. L.; Smith, M. E.; Batsanov, A. S.; Albesa-Jové, D.; Hartl, F.; Howard, J. A. K.; Low, P. J. *Inorg. Chim. Acta* **2006**, *359*, 946−961. (b) Venkatesan, K.; Blacque, O.; Berke, H. *Organometallics* **2006**, *25*, 5190−5200. (c) Qi, H.; Ghupta, A.; Noll, B. C.; Snider, G. L.; Lu, Y.; Lent, C. S. Fehlner, T. P. *J. Am. Chem. Soc.* **2005**, *127*, 15218−15227. (d) Ren, T. *Organometallics* **2005**, *24*, 4854−4870. (e) Sheng, T.; Vahrenkamp, H. *Eur. J. Inorg. Chem.* **2004**, 1198−1203.

(10) Paul, F.; Lapinte, C. *Coord. Chem. Rev.* **1998**, *178/180*, 431−509.

(11) See for instance: Malvolti, F.; Le Maux, P.; Toupet, L.; Smith, M. E.; Man, W. Y.; Low, P. J.; Galardon, E.; Simonneaux, G.; Paul, F. *Inorg. Chem.* **2010**, *49*, 9101−9103.

(12) Grelaud, G.; Tohmé, A.; Argouarch, G.; Roisnel, T.; Paul, F. *New J. Chem.* **2011**, *35*, 2740−2742.

(13) (a) Hegedus, L. S. *Transition Metals in the Synthesis of Complex Organic Molecules*; University Science Books: Mill Valley, CA, 1994. (b) Buchwald, S. L. *Acc. Chem. Res.* **2008**, *41*, 1439−1564.

(14) Allgeier, A. M.; Mirkin, C. A. *Angew. Chem., Int. Ed.* **1998**, *37*, 895−908.

(15) (a) Lorkovic, I. M.; Duff, R. R., Jr.; Wrighton, M. S. *J. Am. Chem. Soc.* **1995**, *117*, 3617−3618. (b) Slone, C. S.; Mirkin, C. A.; Yap, G. P. A.; Guzei, I. A.; Rheingold, A. L. *J. Am. Chem. Soc.* **1997**, *119*, 10743−10743.

(16) For examples of nonferrocene-based ligands, see for instance: (a) Planas, J. G.; Hampel, F.; Gladysz, J. A. *Chem.—Eur. J.* **2006**, *11*, 1402−1416. (b) Scherer, A.; Gladysz, J. A. *Tetrahedron Lett.* **2006**, *47*, 6335−6337. (c) Friedlein, F. K.; Hampel, F.; Gladysz, J. A. *Organometallics* **2005**, *24*, 4103−4105. (d) Kromm, K.; Osburn, P. L.; Gladysz, J. A. *Organometallics* **2002**, *21*, 4275−4280. (e) Eichenseher, S.; Kromm, K.; Delacroix, O.; Gladysz, J. A. *Chem. Commun.* **2002**, 1046−1047 , and refs therein.

(17) For selected examples with ferrocene-based ligands, see: (a) Baupérin, M.; Job, A.; Cattey, H.; Royer, S.; Meunier, P.; Hierso, J.-C. *Organometallics* **2010**, *29*, 2815−2822. (b) Bebbington, M. W. P.; Bontemps, S.; Bouhadir, G.; Hanton, M. J.; Tooze, R. P.; van Rensburg, H.; Bourissou, D. *New J. Chem.* **2010**, *34*, 1556−1559. (c) Marinetti, A.; Voituriez, A. *Synlett* **2010**, *2*, 174−194. (d) Voituriez, A.; Panossian, A.; Fleury-Brégeot, N.; Retailleau, P.; Marinetti, A. *Adv. Synth. Catal.* **2009**, *351*, 1968−1976. (e) Voituriez, A.; Panossian, A.; Fleury-Brégeot, N.; Retailleau, P.; Marinetti, A. *J. Am. Chem. Soc.* **2008**, *130*, 14030−14031. (f) Tschirschwitz, S.; Lönnecke, P.; Hey-Hawkins, E. *Organometallics* **2007**, *26*, 4715−4724. (g) Moslin, R. M.; Jamison, T. F. *Org. Lett.* **2006**, *8*, 455−458. (h) Baillie, C.; Zhang, L.; Xiao, J. *J. Org. Chem.* **2004**, *69*, 7779−7782. (i) Kataoka, N.; Shelby, Q.; Stambuli, P.; Hartwig, J. F. *J. Org. Chem.* **2002**, *67*, 5553−5566. (j) Liu, S.-Y.; Choi, M. J.; Fu, G. C. *Chem. Commun.* **2001**, 2408−2409. (k) *Metallocenes*; Togni, A., Ed.; Wiley-VCH: Weinheim, Germany, 1998. (l) Dietrich, S.; Nicolai, A.; Lang, H. *J. Organomet. Chem.* **2011**, *696*, 739−747.

(18) Jakob, A.; Milde, B.; Ecorchard, P.; Schreiner, C.; Lang, H. *J. Organomet. Chem.* **2008**, *693*, 3821−3830.

(19) Lohan, M.; Milde, B.; Heider, S.; Speck, J. M.; Krausse, S.; Schaarschmidt, D.; Rüffer, T.; Lang, H. *Organometallics* **2012**, *31*, 2310−2326.

(20) Milde, B.; Schaarschmidt, D.; Ecorchard, P.; Lang, H. *J. Organomet. Chem.* **2012**, *706−707*, 52−65.

(21) Milde, B.; Lohan, M.; Schreiner, C.; Rüffer, T.; Lang, H. *Eur. J. Inorg. Chem.* **2011**, *5437−5449*, 52−65.

(22) Schaarschmidt, D.; Kühnert, J.; Tripke, S. S.; Alt, H. G.; Görl, C.; Rüffer, T.; Ecorchard, P.; Walfort, B.; Lang, H. *J. Organomet. Chem.* **2010**, *695*, 1541−1549.

(23) See also for instance: (a) Jakob, A.; Ecorchard, P.; Linseis, M.; Winter, R. F.; Lang, H. *J. Organomet. Chem.* **2009**, *694*, 655−666. (b) Madalska, M.; Lönnecke, P.; Hey-Hawkins, E. *Organometallics* **2013**, *32*, 2019−2025. (c) Sutoh, K.; Sasaki, S.; Yoshifuji, M. *Inorg. Chem.* **2006**, *45*, 992−998. (d) Swartz, B. D.; Nataro, C. *Organometallics* **2005**, *24*, 2447−2451. (e) Barrière, F.; Kriss, R. U.; Geiger, W. E. *Organometallics* **2005**, *24*, 48−52. (f) Nataro, C.; Campbell, A. N.; Ferguson, M. A.; Incarvito, C. D.; Reingold, A. L. *J. Organomet. Chem.* **2003**, *673*, 47−55. (g) Adams, J. J.; Curnow, O. J.; Huttner, G.; Smail, S. J.; Turnbull, M. M. *J. Organomet. Chem.* **1999**, *577*, 44−57. (h) Podlaha, J.; Stepnika, P.; Ludvik, I.; Cisarova, I. *Organometallics* **1996**, *15*, 543−550. (i) Kotz, J. C.; Nivert, C. L.; Lieber, J. M.; Reed, R. C. *J. Organomet. Chem.* **1975**, *91*, 87−95. (j) Kotz, J. C.; Nivert, C. L.; Lieber, J. M.; Reed, R. C. *J. Organomet. Chem.* **1973**, *52*, 387−406.

(24) Baumgartner, T.; Fiege, M.; Pontzen, F.; Arteaga-Müller, R. *Organometallics* **2006**, *25*, 5657−5664.

(25) For TTF-based redox-active phosphine derivatives, see: (a) Lorcy, D.; Bellec, N.; Fourmigué, M.; Avarvari, N. *Coord. Chem. Rev.* **2009**, *253*, 1398−1438. (b) Réthoré, C.; Suisse, I.; Agbossou-Niedercorn, F.; Guillamon, E.; Llusar, R.; Fourmigué, M.; Avarvari, N. *Tetrahedron* **2006**, *62*, 11942−1194 , and refs therein.

(26) Lucas, N. T.; Cifuentes, M. P.; Nguyen, L. T.; Humphrey, M. G. *J. Cluster Sci.* **2001**, *12*, 201−221.

(27) (a) Dahlenburg, L.; Weiss, A.; Bock, M.; Zhal, A. *J. Organomet. Chem.* **1997**, *541*, 465−471. (b) Dahlenburg, L.; Weiss, A.; Moll, M. *J. Organomet. Chem.* **1997**, *535*, 195−200.

(28) Tohmé, A.; Grelaud, G.; Argouarch, G.; Roisnel, T.; Labouille, S.; Carmichael, D.; Paul, F. *Angew. Chem., Int. Ed.* **2013**, *52*, 4445−4448.

(29) Low, P. J. *J. Cluster Sci.* **2008**, *19*, 5−46.

(30) Paul, F.; da Costa, G.; Bondon, A.; Gauthier, N.; Sinbandhit, S.; Toupet, L.; Costuas, K.; Halet, J.-F.; Lapinte, C. *Organometallics* **2007**, *26*, 874−896.

(31) Paul, F.; Toupet, L.; Thépot, J.-Y.; Costuas, K.; Halet, J.-F.; Lapinte, C. *Organometallics* **2005**, *24*, 5464−5478.

(32) Care should be exercised before extending this statement to other organoiron derivatives. For a caveat see ref 28.

(33) Grelaud, G.; Argouarch, G.; Paul, F. *Tetrahedron Lett.* **2010**, *51*, 3786−3788.

(34) Denis, R.; Toupet, L.; Paul, F.; Lapinte, C. *Organometallics* **2000**, *19*, 4240−4251.

(35) Connelly, N. G.; Gamasa, M. P.; Gimeno, J.; Lapinte, C.; Lastra, E.; Maher, J. P.; Le Narvor, N.; Rieger, A. L.; Rieger, P. H. *J. Chem. Soc., Dalton Trans.* **1993**, 2575−2578.

(36) Costuas, K.; Paul, F.; Toupet, L.; Halet, J.-F.; Lapinte, C. *Organometallics* **2004**, *23*, 2053−2068.

(37) Cifuentes, M. P.; Humphrey, M. G.; Morrall, J. P.; Samoc, M.; Paul, F.; Roisnel, T.; Lapinte, C. *Organometallics* **2005**, *24*, 4280−4288.

(38) Paul, F.; Mevellec, J.-Y.; Lapinte, C. *J. Chem. Soc., Dalton Trans.* **2002**, 1783−1790.

(39) Ibn Ghazala, S.; Paul, F.; Toupet, L.; Roisnel, T.; Hapiot, P.; Lapinte, C. *J. Am. Chem. Soc.* **2006**, *128*, 2463−2476.

(40) Paul, F.; Lapinte, C. In *Unusual Structures and Physical Properties in Organometallic Chemistry*; Gielen, M., Willem, R., Wrackmeyer, B., Eds.; Wiley: New York, 2002; p 219−295.

(41) Bertini, I.; Luchinat, C.; Parigi, G. *Solution NMR of Paramagnetic Molecules. Application to Metallobiomolecules and Models*; Elsevier: Amsterdam, The Netherlands, 2001.

(42) Paul, F.; Bondon, A.; da Costa, G.; Malvolti, F.; Sinbandhit, S.; Cador, O.; Costuas, K.; Toupet, L.; Boillot, M.-L. *Inorg. Chem.* **2009**, *48*, 10608−10624.

(43) Grelaud, G.; Cador, O.; Roisnel, T.; Argouarch, G.; Cifuentes, M. P.; Humphrey, M. G.; Paul, F. *Organometallics* **2012**, *31*, 1635−1642.

(44) (a) Intille, G. M. *Inorg. Chem.* **1972**, *4*, 695−702. (b) Fuchs, E.; Keller, M.; Breit, B. *Chem.—Eur. J.* **2006**, *12*, 6930−6939.

(45) Roodt, A.; Otto, S.; Steyl, G. *Coord. Chem. Rev.* **2003**, *245*, 121−137 , and refs therein.

(46) In line with discrepancies present in the literature regarding the reported energy of the ν_{CO} mode of **17**,[47,48] we have presently checked that a significant difference exists, depending if the measurement is conducted in CH_2Cl_2 solution (1978 ± 2 cm^{-1})[45,48,49] or in the solid state (1963 ± 2 cm^{-1}).[50,51] For all compounds, higher values were always obtained in solution (CH_2Cl_2). In line with the recommendations of Roodt et al.,[45] we have based our discussion on these values that we consider free of solid-state effects.

(47) Moloy, K. G.; Petersen, J. L. *J. Am. Chem. Soc.* **1995**, *117*, 7696−7710.

(48) Pickett, T. E.; Roca, F. X.; Richards, C. J. *J. Org. Chem.* **2003**, *68*, 2592−2599.

(49) Otto, S.; Roodt, A. *Inorg. Chim. Acta* **2004**, *357*, 1−10.

(50) Dunbar, K. R.; Haefner, S. C. *Inorg. Chem.* **1992**, *31*, 3676−3679.

(51) (a) Clarke, M. L.; Cole-Hamilton, D. J.; Slawin, A. M. Z.; Woollins, J. D. *Chem. Commun.* **2000**, 2065−2066. (b) Gulyas, H.; Bacsik, Z.; Szollosy, A.; Bakos, J. *Adv. Synth. Catal.* **2006**, *348*, 1306−1310.

(52) Tolman, C. A. *Chem. Rev.* **1977**, *77*, 313−348.

(53) (a) Otto, S. *J. Chem. Crystallogr.* **2001**, *31*, 185−190. (b) Otto, S.; Roodt, A.; Smith, J. *Inorg. Chim. Acta* **2000**, *303*, 295−299.

(54) (a) Muller, A.; Otto, S.; Roodt, A. *Dalton Trans.* **2008**, 650−657. (b) Chevykalova, M. N.; Manzhukova, L. F.; Artemova, N. V.; Luzikov, Y. N.; Nifanťev, I. E.; Nifanťev, E. E. *Russ. Chem. Bull.* **2003**, *52*, 78−84 , and refs therein.

(55) Courmarcel, J.; Le Gland, G.; Toupet, L.; Paul, F.; Lapinte, C. *J. Organomet. Chem.* **2003**, *670*, 108−122.

(56) (a) Makowska-Janusik, M.; Kityk, I. V.; Gauthier, N.; Paul, F. *J. Phys. Chem. C* **2007**, *111*, 12094−12099. (b) Costuas, K.; Cador, O.; Justaud, F.; Le Stang, S.; Paul, F.; Monari, A.; Evangelisti, S.; Toupet, L.; Lapinte, C.; Halet, J.-F. *Inorg. Chem.* **2012**, *50*, 12601−12622. (c) Drouet, S.; Merhi, A.; Grelaud, G.; Cifuentes, M. P.; Humphrey,

M. G.; Matczyszyn, K.; Samoc, M.; Toupet, L.; Paul-Roth, C. O.; Paul, F. *New J. Chem.* **2012**, *36*, 2192−2195. (d) Trujillo, A.; Veillard, R.; Argouarch, G.; Roisnel, T.; Singh, A.; Ledoux, I.; Paul, F. *Dalton Trans.* **2012**, *41*, 7454−7456.

(57) Allen, F. H.; Kennard, O.; Watson, D. G.; Brammer, L.; Orpen, A. G.; Taylor, R. *J. Chem. Soc., Perkin Trans.* **1987**, *2*, S1−S19.

(58) See for instance: Muller, A.; Otto, S. *Acta Crystallogr., Sect. C* **2011**, m165−m168 and refs therein.

(59) Orpen, A. G.; Brammer, L.; Allen, F. H.; Kennard, O.; Watson, D. G.; Taylor, R. *J. Chem. Soc., Dalton Trans.* **1989**, S1−S83.

(60) Hansch, C.; Leo, A.; Taft, R. W. *Chem. Rev.* **1991**, *91*, 165−195.

(61) (a) Brown, T. L.; Lee, K. J. *Coord. Chem. Rev.* **1993**, *128*, 89−116. (b) White, D.; Coville, N. J. *Adv. Organomet. Chem.* **1994**, *36*, 95−158. (c) White, D.; Taverner, B. C.; Coville, N. J.; Wade, P. W. *J. Organomet. Chem.* **1995**, *495*, 41−51. (d) Smith, J. M.; Taverner, B. C.; Coville, N. J. *J. Organomet. Chem.* **1997**, *530*, 131−140.

(62) Müller, T. E.; Mingos, D. M. P. *Transition Met. Chem.* **1995**, *20*, 533−539.

(63) Verkade, J. G.; Mosso, J. A. In *Organic Compounds and Metal Complexes*; Verkade, J. G., Quin, L. D., Eds.; VCH: Weinheim, Germany, 1987; pp 453−455.

(64) Gauthier, N.; Olivier, C.; Rigaut, S.; Touchard, D.; Roisnel, T.; Humphrey, M. G.; Paul, F. *Organometallics* **2008**, *27*, 1063−1072.

(65) Sollott, G. P.; Mertwoy, H. E.; Portnoy, S.; Snead, J. L. *J. Org. Chem.* **1963**, *28*, 1090−1092 , and refs therein.

(66) (a) Ge, Q.; Corkery, T. C.; Humphrey, M. G.; Samoc, M.; Hor, T. S. A. *Dalton Trans.* **2009**, 6192−6200. (b) Ge, Q.; Dalton, G. T.; Humphrey, M. G.; Samoc, M.; Hor, T. S. A. *Asian Chem. J.* **2009**, *4*, 998−1005.

(67) Shriver, D. F.; Drezdzon, D. E. *The Manipulation of Air-Sensitive Compounds*; Wiley and Sons: New York, 1986.

(68) Fulmer, G. R.; Miller, A. J. M.; Sherden, N. H.; Gottlieb, H. E.; Nudelman, A.; Stoltz, B. M.; Bercaw, J. E.; Goldberg, K. I. *Organometallics* **2010**, *29*, 2176−2179.

(69) Connelly, N. G.; Geiger, W. E. *Chem. Rev.* **1996**, *96*, 877−910.

(70) Roger, C.; Hamon, P.; Toupet, L.; Rabaâ, H.; Saillard, J.-Y.; Hamon, J.-R.; Lapinte, C. *Organometallics* **1991**, *10*, 1045−1054.

(71) Altomare, A.; Burla, M. C.; Camalli, M.; Cascarano, G.; Giacovazzo, C.; Guagliardi, A.; Moliterni, A. G. G.; Polidori, G.; Spagna, R. *J. Appl. Crystallogr.* **1999**, *32*, 115−119.

(72) Sheldrick, G. M. *SHELX97-2, Program for the refinement of crystal structures*; University of Göttingen: Göttingen, Germany, 1997.

(73) Farrugia, L. J. *J. Appl. Crystallogr.* **1999**, *32*, 837−838.

(74) Sluis, P. v. d.; Spek, A. L. *Acta Crystallogr.* **1990**, *A46*, 194−201.

(75) Spek, A. L. *Appl. Crystallogr.* **2003**, *36*, 7−13.

(76) Reidel, D. *International Tables for X-ray Crystallography*; Kynoch Press (present distrib. D. Reidel, Dordrecht): Birmingham, U.K., 1974; Vol. *IV*.